TOWARDS ALUMINIUM INJECTION MOULDING FOR AUTOMOTIVE PARTS

ATSAWIN SALEE

A THESIS SUBMITTED IN PARTIAL FULFILLMENT

OF THE REQUIREMENT FOR THE DEGREE OF

MASTER OF ENGINEERING IN AUTOMOTIVE ENGINEERING

(INTERNATIONAL PROGRAM)

INTERNATIONAL COLLEGE

KING MONGKUT'S INSTITUTE OF TECHNOLOGY LADKRABANG

2009

KMITL-2009-IC-M-004-001

Thesis Title	Towards Aluminium Injection Moulding for Automotive Parts
Student	Mr. Atsawin Salee
Student ID.	50061901
Degree	Master of Engineering
Program	Automotive Engineering (International Program)
Year	2009
Thesis Advisor	Assoc. Prof. Dr. Chinaruk Thianpong
	Dr. Anchalee Manonukul
	Assoc. Prof. Dr. Kunio Takahashi

ABSTRACT

This work is the first step towards aluminium injection moulding process by studying the process ability of aluminium alloy through the compaction and sintering process. The starting material was the Al-Si-Cu-Mg alloy powder containing Si and Cu as the alloying elements and Mg as the sintering aid. This work was divided into two parts. The first part concerned to the effects of sintering conditions on the sinterability of Al-Si-Cu-Mg alloy. In this part, the aluminium alloy powder was compacted into the tensile test specimens with the average green density of 2.50 g/cm^3. Those green specimens were sintered in four sintering conditions, in which the purity of nitrogen, the level of vacuum applied before sintering, the control atmosphere, and the sintering chamber, were adjusted. However, dewaxing and sintering temperature profile was set to be the same in all sintering conditions. It was found that sintering by using the flow controlled 99.999% purity of nitrogen atmosphere with appropriate gas flow rate in the tubular furnace, produced the best sintered properties. This condition gave the lowest atmosphere dew point and hence enhanced sintering of aluminium alloy powder because it was found that there was the reduction of oxygen per aluminium content after sintering when compared with the green stage. The second part was to study the effects of compaction pressures on the sinterability of aluminium alloy by applying compaction pressures varied from 150 to 700 MPa. The green specimens were sintered by using the best sintering condition obtained from the first sub-experiment. It was found that the sintered properties were decreased as the compaction pressure decreased. The main cause of decreasing in densities and properties was the self-gettering

phenomenon, which was more pronounced at lower compaction pressure. This caused a thicker layer of pores remained and distributed at the superficial region.

ACKNOWLEDGEMENT

This thesis could not be completed without the assistance of many persons to whom I would like to express my sincere appreciation.

First, I would like to sincerely thank my advisor, Dr. Anchalee Manonukul, who has given me many helpful suggestions, useful advice and fruitful discussions during the undertaken research.

I would also like to sincerely thank Assoc. Prof. Dr. Chinaruk Thianpong for kind advising and helping, and Assoc. Prof. Dr. Kunio Takahashi for the suggestion of oxide analysis.

Moreover, I would like to acknowledge ECKA Granulate, GmbH, Germany, for supplying the aluminium alloy powder as well as technical advising, that was very useful for improvement this research work. I would like to show gratitude to National Metal and Materials Technology Center (MTEC), especially the metal injection moulding (MIM) laboratory for providing the laboratory equipments and instruments as well as financial supporting.

I am grateful to National Science and Technology Development Agency (NSTDA), which provided the full scholarship for studying in the master program.

Special thanks go to MTEC MIM laboratory's members for helping me during the experiment.

Finally, I am very grateful to my family for all love, caring, understanding and motivation throughout my life.

Atsawin Salee

CONTENTS

CONTENTS (CONT.)

CONTENTS (CONT.)

LIST OF TABLES

LIST OF FIGURES

LIST OF FIGURES (CONT.)

LIST OF FIGURES (CONT.)

CHAPTER 1

INTRODUCTION

1.1 Significance and Background

Increasing demand for lightweight components, primarily driven by the need to reduce energy consumption, has led to increase usage of aluminum especially for the automotive components. Aluminium and its alloys are used in several automotive parts, including sliding and frictional parts. Therefore, the high wear resistant components, such as aluminium silicon alloy (Al-Si alloy), are mostly required (Vukcevic and Delijic, 2002). Additionally, the most common process to fabricate those components is casting, for example sand casting, investment casting, or pressure die casting. However, the automotive components are usually fabricated in large quantities, therefore sand casting and investment casting are limited because non-permanent moulds are used and the quality control is difficult. In addition, although the permanent mould is used in pressure die casting, the high temperature of molten metal is the limited factor of the mould life and dimensional accuracy. Casting is also limited and non-economical if parts are small and complex, especially very thin.

Powder metallurgy (P/M) is the near net-shape metal forming process that transforms the metallic powder into finished components by the application of pressure and heat. P/M process is competitively economic process for the large volume production. However, the components commercially fabricated through this process are commonly made of ferrous metals. Non-ferrous metal, such as aluminium and its alloy are still in an experimental stage due to the presence of its stable oxide layer that always covers the powder surface. This oxide will prevent the particle bonding during sintering and hence will cause the poor sinterability.

In order to achieve good sintering of aluminium, therefore, the oxide should be reduced and/or ruptured before and/or during sintering. There have been a limited number of researches focusing on techniques to reduce and/or rupture the oxide layer covering the powder surface and hence enhance sinterability such as (1) vacuum processing (Flumerfelt, 1999; Griffith *et al.*, 1986; Pickens, 1981), (2) powder coating (Ciomek, 1991; Hu, 1995), (3) applying high compaction pressure (Andreeva and Rastrigina, 1966; Gutin *et al.*, 1972), and (4) using sintering

aids or alloying (Fuentes *et al.*, 2003; Lumley *et al.*, 1999; Schaffer *et al.*, 2001; Schaffer, 2004; Sercombe and Schaffer, 1999; Sercombe, 2003).

There was one previous work on the processing of Al-Si P/M alloy by using vacuum processing (Yilmas and Altintas, 1996), but it was found that it was not feasible to obtain high density. The alternative process with a high compaction pressure, such as the pressure-assisted sintering was required in order to obtain high density. However, it was found that the sinterability of this aluminium alloy was improved by using of sintering aids (LaDelpha *et al.*, 2002).

Not only the sintering aids that improved the sinterability of aluminium, but also the processing parameters. Atmosphere dew point was found to be the most important parameter in the sintering process of aluminium. Sintering of aluminium requires the lower atmosphere dew point than sintering of ferrous metal (German, 1996), which can not physically attain in the conventional sintering furnace. The effects of this parameter on the sinter ability of aluminium were not clear in previous works (Dudas and Dean, 1969; Schaffer *et al.*, 2006) and there was no systematic study about this parameter.

Therefore, this work would like to investigate in the effects of atmosphere dew point on the sinterability of Al-Si-Cu-Mg alloy that contained Mg as the sintering aids. The effects of atmosphere dew point were studied by adjusting sintering conditions. In addition, from the previous work, it was also found that compaction pressure can improve the sintered density (Yilmas and Altintas, 1996). Hence, the effects of compaction pressures on the sinterability of Al-Si-Cu-Mg alloy were also investigated.

1.2 Objectives

1.2.1 To study the effects of sintering conditions on process ability of Al-Si-Cu-Mg alloy.

1.2.2 To study the effects of compaction pressure on process ability of Al-Si-Cu-Mg alloy.

1.3 Scopes

1.3.1 The first study was on the compaction and sintering process of the aluminium alloy powder by using the sintering aids technique under various sintering conditions. In

this work, an example grade of aluminium alloy powder, that used in automotive parts, was selected. The pressing process was employed primary to shape the powder into the tensile test specimens. Consequently, these specimens were sintered in various sintering conditions and then studied their physical and mechanical properties.

1.3.2 The second study was on the sinterability of aluminium alloy by varying compaction pressure. The specimens after compaction using various pressures were sintered using the optimum condition from the sintering condition study and hence their sintered properties were evaluated.

1.4 Expected Benefits

1.4.1 Understanding the processing method for aluminium parts through the powder metallurgical process.

1.4.2 Understanding the process mechanism occurred during sintering.

1.4.3 Being able to use the basic scientific equipments and characterising instruments for material science and engineering study.

1.4.4 Useful research works which can be extended to the actual application in the automotive industries or more advanced applications.

CHAPTER 2

LITERATURE REVIEWS

2.1 Introduction to Aluminium Powder Metallurgy (Al-P/M)

Aluminium and its alloys are currently favourable for applications that need lightweight, high-strength-to-weight ratio, good electrical and thermal conductivity, and excellent corrosion resistance (Apelian and Saha, 2000). Especially in automotive industries, there are high consumption of aluminium in order to reduce the automobile weight and lead to reduce the fuel consumption (Carpenter, 2000). Additionally, the cost of part fabrication together with its reliability has led to develop the net-shaped manufacturing process, known as powder metallurgy (P/M).

The advantages of aluminium P/M lie in the inherent advantages of the powder metallurgical process. P/M is a net-shaped manufacturing process, whereby the solid metal and alloys in the form of small particle or powder is converted to the nearly finished or finished parts by mechanical and thermal consolidation. Die compaction or pressing process is the first and most common forming process for P/M. Hence, die compaction is also known as the conventional P/M process. The basics steps consist of the powder preparation, the compaction of loosed powder into a handleable specimen, and sintering or heating the compacted specimen in a controlled atmosphere and at a temperature below the melting point of the major constituent. The conventional P/M process is cost effective in producing relatively complex parts with only minor secondary operations if necessary. Parts like cam, gear, sprocket, and pulley can be economically produced (Delarbre and Kerhl, 2000; Jangg *et al.*, 1996).

Apart from the conventional P/M process, there is another forming process that has been recently interesting for the production of small and very complex parts, namely metal injection moulding (MIM) process. For MIM, the metallic powders have to be transformed into a mouldable state by mixing the metallic powders with the polymeric binder. This binder will make the powder flowable in an injection moulding machine under the moulding condition. After moulding, the binder has to provide the shape stability and strength for the moulded part (Thummler and Oberacker, 1988). The subsequent step, called debinding, is to remove the binder, which leaves the skeleton of metallic powder. The process is finally completed by

sintering similar to the conventional P/M process. The major difference between the conventional P/M and MIM processes is he forming steps. In the conventional P/M process, the specimen is formed in the compacted solid using a high pressure. However in MIM, the specimen is shaped in fluid-like form by less pressure. Hence, it is possible to inject parts with higher shape complexity than the conventional P/M (German and Bose, 1997). Another difference between those two processes is that MIM process needs the debinding process prior to enter the sintering process, while the conventional P/M process can omit the debinding by directing to the sintering process.

Currently, the aluminium part fabrication through the P/M process is an on-going research and developing stage because sintering of aluminium is difficult. This is due to the oxide layers that always present and cover the powder surface and hence they will act as the sintering barrier that prevents any mass transport event during sintering. Therefore, these layers have to be reduced or ruptured in order to enable and enhance sinterability of aluminium.

2.2 Oxide and the Techniques to Reduce or Rupture the Oxide Layers in Aluminium P/M

2.2.1 Oxide of Aluminium Powder

Aluminium powder is always covered by the oxide layers if it comes into content with oxygen, for example, in air and water. The thickness of the oxide layers is varied depending on the powder production process and the post-production handling and storage atmosphere. For the atomisation process, the oxide layer thickness was initially 5 Å on the molten droplet. The residual water in the atomising gas and spray chamber was chemisorbed into the oxide layers and physiosorbed onto the surface oxide layers (Flumerfelt, 1999). In addition, the oxide thickness was also dependent on the types of atomising agents, for example air and inert gases. It was found that the oxide thickness calculated from the air-atomised aluminium powder was significantly higher than that calculated from the gas atomised powder (Gorner and Forster, 1995). In addition to the gas atomisation, the atomising gas with different physical properties, such as density, thermal conductivity, and flow properties, also affected the oxide thickness of the atomised aluminium powder (Ozbilen *et al.*, 2000).

However, if the oxide thickness had not reached it saturated value, oxidation continued during post-atomisation handling until the oxide thickness had grown to a saturated

value. The rate of oxidation of the post-atomised aluminium powder directly depended on the atmosphere humidity and temperature at which the powder was stored (Kim *et al.*, 1996; Neikov and Krajnikov, 1996).

2.2.2 Techniques to Reduce or Rupture the Oxide Layers in Aluminium P/M

Sintering of aluminium is impeded by the presence of oxide layers. To facilitate sintering, these layers have to be reduced or ruptured. Consider the oxidation and reduction of a metal (M), which is in equilibrium with oxygen and its oxide (M_xO_2) shown in Equation (2.1) (German, 1996). The subscript represents the stoichiometry of the oxide. The bracket shows the matter state, which is g for gas and s for solid.

$$xM\,(s) + O_2\,(g) \leftrightarrow M_xO_2\,(s) \tag{2.1}$$

The free energy is given by:

$$\Delta G = -RT \ln k_1 \tag{2.2}$$

where T is the absolute temperature, R the gas constant and k_1 the equilibrium constant given by:

$$k_1 = (P_{O_2})^{-1} \tag{2.3}$$

where P_{O_2} is the oxygen partial pressure. By substituting Equation (2.3) into Equation (2.2) yields,

$$\Delta G = RT \ln(P_{O_2}) \tag{2.4}$$

In addition, the atmosphere containing hydrogen is often used in P/M to reduce the metal oxide (Lumley *et al.*, 1999) by:

$$MO\,(s) + H_2\,(g) \leftrightarrow M\,(s) + H_2O\,(g) \tag{2.5}$$

The equilibrium constant for this reaction, k_2, is given by:

$$k_2 = \frac{P_{H_2O}}{P_{H_2}} \tag{2.6}$$

where P_{H_2O} and P_{H_2} are the partial pressures of water vapour and hydrogen respectively. Therefore, by the similar way to Equation (2.4), the free energy can be represented by:

$$\Delta G = -RT \ln\left(\frac{P_{H_2O}}{P_{H_2}}\right) \tag{2.7}$$

The ratio of water and hydrogen partial pressure can be converted to dew point, which relates to the water vapour content. From Equations (2.4) and (2.7), it was found that for aluminium sintered at 600°C, an oxygen partial pressure, P_{O_2}, of less than 10^{-50} atm or a dew point of less than -140°C was required in order to reduce aluminium oxide (Lumley *et al.*, 1999). Neither of these is physically attainable in practical sintering process. Therefore, other mechanisms of oxide reducing or rupturing are required.

From literature reviews, there have been four techniques to reduce or rupture the oxide layers of aluminium powder during processing. More detail of each technique is described next.

2.2.2.1 Vacuum Processing

Vacuum processing is the reducing technique. As aforementioned that an oxygen partial pressure of less than 10^{-50} atm is required to reduce the oxide (Lumley *et al.* 1999). It is over the ultrahigh vacuum level, which cannot probably be reached in a conventional furnace. In practice, the ultrahigh level of vacuum used in Al-P/M is to minimise reaction with contaminants and prevent as much as possible Al from further oxidation. In addition, vacuum processing can be applied to treat the powder before consolidating, this process is known as degassing. Degassing is always operated with the hot forming process, for example hot forging of hot isostatic pressing (Pickens, 1981). Powder should be degassed at a temperature below the consolidation temperature. Degassing is carried out in order to remove the adsorbed species such as oxygen or water, which come from the atomisation and handling (Thummler and Oberacker, 1993). The surface oxide layers on aluminium and aluminium alloy powders contain aluminium oxide and aluminium hydroxides. During degassing of the aluminium powders, by products such as moisture, adsorbed hydrogen, and oxygen are removed, the hydroxides are decomposed, and the ductile amorphous aluminium hydroxide is transformed into the brittle crystalline γ-alumina according to the reaction below (Flumerfelt, 1999; Griffith *et al.*, 1986; Kim *et al.*, 2000);

$$Al_2O_3 \cdot 3H_2O \xrightarrow[450-580K]{} Al_2O_3 \cdot H_2O + 2H_2O\uparrow \xrightarrow[800-820K]{} \gamma\text{-}Al_2O_3 + H_2O\uparrow \qquad (2.6)$$

Although the final yield of the degassing process is not the pure aluminium, it is the brittle aluminium oxide (γ-Al_2O_3) which can be broken away easily during further consolidation such as pressing or forging.

2.2.2.2 Applying High Compaction Pressure

During compaction step, the powders have to be deformed plastically to retain the overall shape of the specimen after ejecting from a die. During plastic deformation of aluminium powders, the oxide layers are ruptured, resulting in the local areas of contact between the particles are free from oxide (Gutin *et al.* 1972). Subsequently during sintering, the diffusion of atoms takes place through these oxide-free interfaces. Thus, the higher compaction pressure, the sintering operation is more effective.

2.2.2.3 Powder Coating

The concept of this technique is to cover an aluminium powder with a less reactive metal. The selection of the less reactive metal is based on an alloying element that always presents with aluminium such as copper, zinc, or nickel (Ciomek, 1991). In order to achieve this technique, the reactive metal powder, i.e. aluminium powder should be processed to ensure that its oxide layers are simultaneous removal, while the less reactive metal is simultaneously deposited on the powder surface. The mentioned process is the electroless plating, which is the usual coating technique for the reactive metal such as magnesium, aluminium, and titanium (Gray and Luan, 2002).

Coating by electroless plating has two main steps (Djokic *et al.*, 1999; Tomolya *et al.*, 2005). The first step is the surface preparation. In this step, the metal powder as substrate will be dispersed in an alkaline ammonical solution to remove impurities, activate the powder surface and readily receive the subsequent coating step. The second step is coating by addition of the reducing agent and coating media solution in the form of salt solution. For example, if the copper-coated aluminium powder is prepared, the copper salt solution such as the copper sulphate solution is needed in the coating step as the coating media. The displacement reaction takes place at the active surface of powder. After enough coating, the solution is

decanted and the powder is filtered and washed with deionised water to pH 7 and finally dried at temperature range of 100-105°C.

Ciomek (1991) prepared the aluminium powder having copper coating for metal injection moulding of aluminium powder. In his work, the aluminium powder was added into the prepared cupric salt solution. The coating reaction was controlled through the pH value of the cupric salt solution. Ciomek (1991) suggested that it was advantageous to use a cupric salt solution that has a pH above 7 to provide a reaction that was easily controlled. In addition, the nickel coated aluminium powder was prepared by Hu (1995). The nickel chloride solution was used as the coating media for aluminium powder.

2.2.2.4 Using of Sintering Aids

The main concept of this technique is based on the reduction mechanism by adding another element that is more reactive to oxygen than aluminium into an aluminium powder system. It was found that the addition of magnesium (Mg) in the aluminium powder system could reduce the aluminium oxide to reveal the underlying aluminium atoms and facilitate sintering (Fuentes *et al.*, 2003; Lumeley *et al.*, 1999).

Magnesium can reduce the oxide of aluminium resulting in formation of two species, $MgAl_2O_4$ (Spinel) and magnesium oxide (MgO). The forming reactions of these two species are shown as followed (Kimura *et al.*, 2001; McLeod and Gabryel, 1992):

$$3Mg + 4Al_2O_3 \rightarrow 3MgAl_2O_4 + 2Al;\ \Delta G_{800K} = -280kJ/mol \quad (2.7)$$

$$3Mg + Al_2O_3 \rightarrow 3MgO + 2Al;\ \Delta G_{800K} = -136kJ/mol \quad (2.8)$$

However, these formations depend on the magnesium content and temperature, which they are formed as observed by Xie *et al.* (2005). In aluminium rich magnesium alloy, MgO is dominantly occurred, while $MgAl_2O_4$ is dominantly occurred in aluminium lean magnesium alloy at the experimental temperature. However, at the critical content of magnesium, there is a change between MgO to $MgAl_2O_4$ with an increasing experimental temperature (Xie *et al.*, 2005).

Lumley *et al.* (1999) concluded about the reduction mechanism of aluminium oxide by the addition of magnesium and represented the reduction mechanism as shown in Figure 2.1. It shows that at the Mg-oxide contact site, local MgO can occur due to the

relative rich of magnesium. Magnesium diffuses along the metal-oxide interface and through the aluminium powder and then reduces the oxide at the metal-oxide interface. Nearby aluminium particles, which are not directly in contact with magnesium powder, are subsequently exposed to the reductance and their oxide layers are disrupted.

In addition, for the pre-alloyed powder of aluminium containing magnesium as an alloying element, the dissolved magnesium in the powder particles migrates into the surface oxide and is saturated in the composition where the Mg/Al ratio is about 0.5 during heating. When the sintering temperature is reached, magnesium reduces aluminium oxide at the particle surfaces, resulting in the breakage of the surface oxide layers and eventually appearance of metallic aluminium on the outer surface of the powder particles (Kimura *et al.*, 2001). Figure 2.2 (a) shows the TEM observation at the region of bonding interface between two particles of aluminium alloy containing 0.3% wt. of magnesium. The corresponding high magnification image in Figure 2.2 (b) was taken from the square frame as shown in Figure 2.2 (a). Figure 2.2 (b) shows the Al-Mg grain at left and right-hand side and a lot of precipitates observed at the interface. Therefore, further analysis by EDS was taken at these specific areas, designated as *A*, *B*, and *C* in Figure 2.2 (b). The results are found that at the area *A*, the peaks of oxygen, aluminium and magnesium were observed, which were more likely to be $MgAl_2O_4$. While the areas *B* and *C* were observed to be Al-Mg matrix and pure Al respectively (Xie *et al.*, 2005).

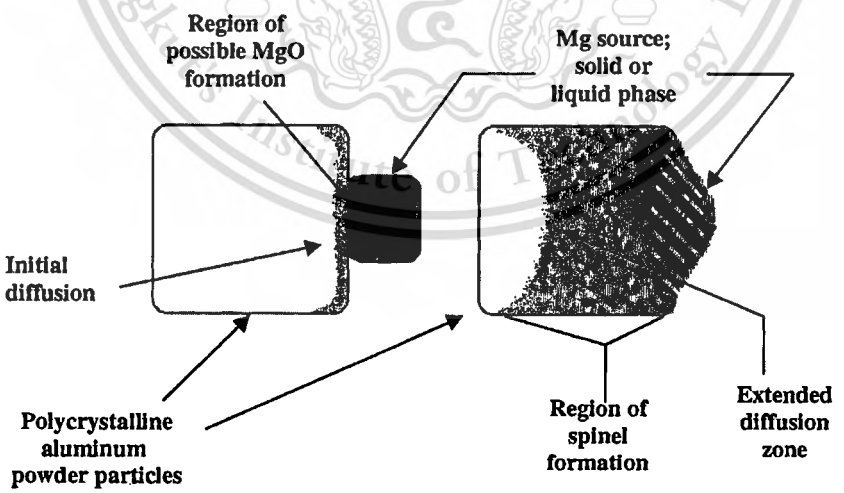

Figure 2.1 A schematic representation of the processes involved in the reduction of the alumina layer by magnesium during the sintering of Al-Mg alloys (Lumley *et al.*, 1999).

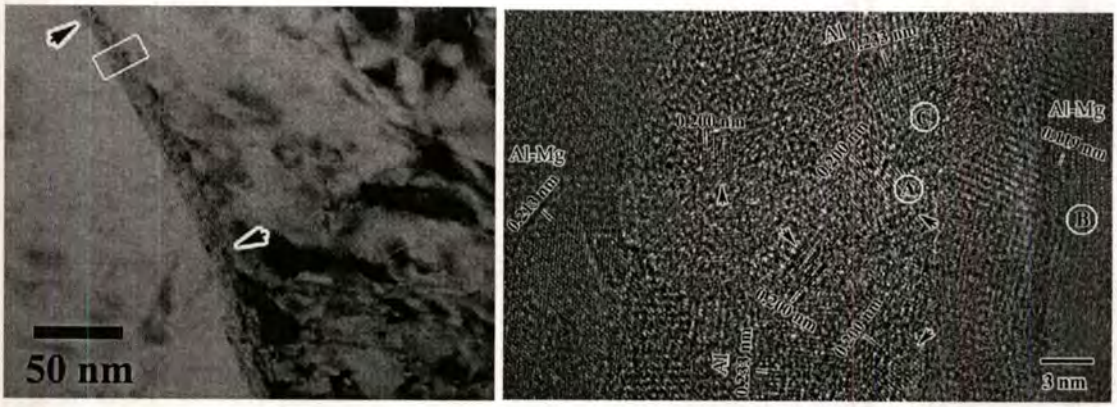

(a) (b)

Figure 2.2 TEM micrographs of Al–0.3Mg alloy specimen, (a) a bright-field TEM image, (b) corresponding high magnification TEM image taken from the square frame in (a), which is the interface region of bonding (Xie *et al.*, 2005).

Apart from magnesium that plays an important role in the reduction mechanism, there are other sintering aids that can be added into an aluminium system in which based on the common alloying elements that always presented with aluminium, namely copper (Cu), zinc (Zn), and silicon (Si). These elements play a role in formation of liquid phase during sintering (Schaffer *et al.*, 2001). Sercombe (1998) stated about the role of liquid phase forming during sintering that the eutectic liquid could penetrate the oxide layers at the crack caused by compaction. The melt could then diffuse through the cracks, lifted the oxide layers and allowed metal-metal bonding to occur. Moreover, when the additive phase became solid solubility in aluminium, expansion caused by diffusion of these elements into solution may cause oxide fracture.

Although sintering with the presence of sintering aids seems to have expansion of the specimen by the diffusion of those additives into aluminium matrix, shrinkage during sintering is also occurred by the mechanism of liquid phase sintering itself (German, 1996; Schaffer *et al.*, 2008).

2.2.3 Comparison of Techniques to Reduce and Rupture the Oxide Layers in Al P/M

For P/M processing of aluminium, there have been four techniques to reduce or rupture the oxide layers of aluminium as reviewed above and can be summarised for comparison in Table 2.1. The vacuum processing and powder coating techniques are the oxide reducing

technique and hence lower oxygen contents were observed in the specimens. On the other hand, the applying high compaction pressure technique is the oxide rupturing technique by which the oxide is ruptured during deformation. While both reducing and rupturing mechanisms are active in the using of sintering aids technique.

The vacuum and applying high compaction pressure techniques can produce both pure aluminium and aluminium alloy, while pure aluminium parts cannot be fabricated by the powder coating and sintering aids techniques because of the addition of coating material or sintering aids elements respectively. However, the additional alloying elements can also be tailored to improve the required final properties.

The vacuum processing, applying high compaction pressure, and powder coating techniques increase the cost of production because these techniques require additional process or special equipment or machine. Whereas the low production cost can be obtained by using the sintering aids technique because the alloying of aluminium is commonly done in P/M, hence it utilises the current P/M equipments without additional process.

Table 2.1 Comparison of each oxide reducing or rupturing technique.

Technique	Material		Mechanism	Cost
	Pure Al	Al Alloy		
1. Vacuum processing (Flumerfelt, 1999; Griffith *et al.*, 1986; Kim *et al.*, 2000; Pickens, 1981)	✓	✓	Reducing oxide	High
2. High compaction pressure (Andreeva and Rastrigina, 1965; Gutin *et al.*, 1972)	✓	✓	Rupture oxide	High
3. Powder coating (Ciomek, 1991; Hu, 1995)	✗	✓	Reducing oxide	High
4. Sintering aids (Fuentes *et al.*, 2003; Lumley *et al.*, 1999; Schaffer *et al.*, 2001; Schaffer, 2004; Sercombe and Schaffer, 1999; Sercombe, 2003)	✗	✓	Reducing and Rupturing oxide	Low

In addition, it is found that all techniques have been originally applied in conventional P/M process. There have been works on aluminium injection moulding that applies some techniques in order to achieve good sinterability, for example, Tan, Ma (2004) applied the vacuum processing technique, and Ciomek (1991) applied the powder metal coating. However, the processing details of these two works are not clarified and they are kept as a trade secret.

From the comparison of each technique in Table 2.1, it is found that the sintering aids technique is outstanding because this technique is simple and can utilise the current P/M equipments. In addition, this technique has not been adapted for MIM before. In the vacuum processing technique, all machines have to be modified to carry the processing under vacuum especially during mixing. Furthermore, the additional degassing process has to be done prior to shaping or sintering, which relates to the additional cost. For the powder coating technique, an additional powder coating process is necessary before compaction or injection. Moreover, the high pressure compaction technique as its name suggests requires high pressure equipments.

2.3 Parameters in Sintering of Aluminium with the Addition of Sintering Aids

2.3.1 The Effects of Sintering Aids

Although magnesium is a common reducing agent during sintering of aluminium, there is still the limitation of magnesium addition. It was found that the maximum content less than 1% by weight of magnesium could reduce the oxide through the formation of spinel ($MgAl_2O_4$), but this was dependent on the aluminium particle size as shown in Figure 2.3 (Lumley *et al.*, 1999). It shows that more magnesium was required to sinter smaller powders because of the greater surface area and hence more amount of oxide. Furthermore, the addition of more than 1% by weight caused the net expansion of specimens as shown in Figure 2.4. This is due to the excess magnesium diffused into the base metal, especially from the liquid phase (Fuentes *et al.*, 2003; Lumley *et al.*, 1999).

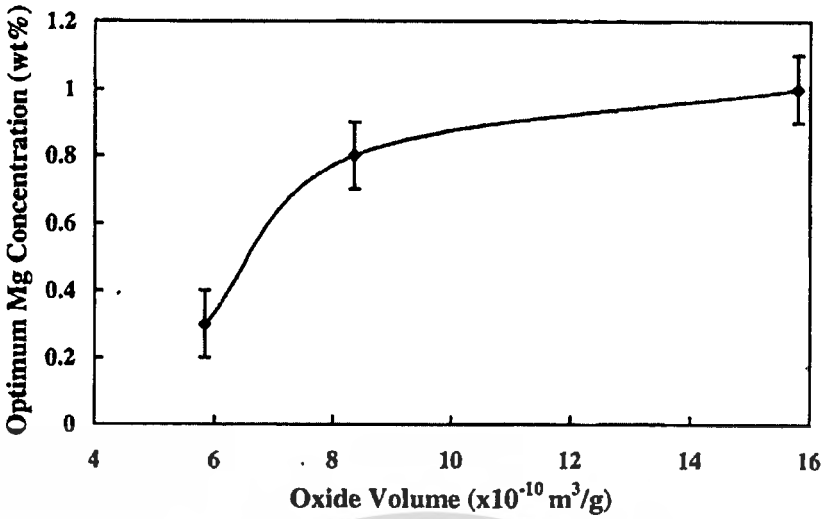

Figure 2.3 The concentration of magnesium required to achieve maximum densification in binary aluminium-magnesium alloy as a function of oxide volume (Lumley *et al.*, 1999).

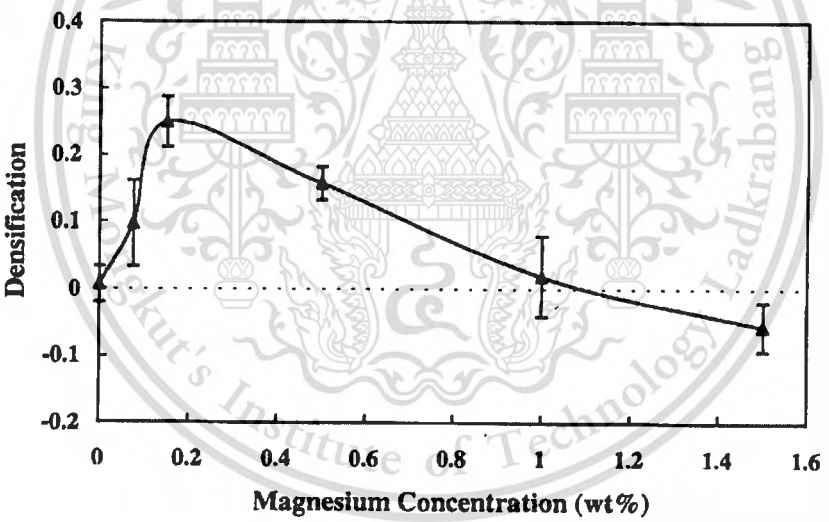

Figure 2.4 The effect of magnesium on the densification of aluminium powder. The densification[1] was maximised at 0.15% wt. of Mg, and there was net expansion at concentrations more than 1% by weight (Lumley *et al.*, 1999).

[1] Densification is a parameter that indicates the ability to densify of the sintered compact relative pore free compact from its green stage (German, 1996). Densification value is given by $\psi = \frac{\rho_s - \rho_g}{\rho_t - \rho_g}$, where ρ_s is the sintered density, ρ_g the green density, and ρ_t the theoretical density. The positive value indicates there is shrinkage occurred while negative value indicates expansion.

Copper (Cu) is one of the primary alloying elements for aluminium and can be used as sintering aid. The major influence of copper is on the tensile properties of sintered aluminium (Schaffer, 2004). Sintering of aluminium with copper always occurred in transient liquid phase sintering (Schaffer *et al.*, 2001), in which total Cu in the liquid solution is drawn into the aluminium and when Cu is completely dissolved, the liquid solution is disappeared. However, the major problem in sintering of aluminium-copper alloy system is the diffusivity of copper in aluminium is 5000 times than that of aluminium in copper and hence causes the expansion of the sintered specimen. Therefore, sintering of the Al-Cu system should be carefully controlled and is dependent on the process variables.

Silicon (Si) is another possible sintering aid that always presented as a major alloying element in the 6xxx series alloy, and a minor addition in the 2xxx series alloy. In 6xxx series alloy, silicon enhances the sinterability through the formation the liquid phase with aluminium and magnesium (Showaiter and Youseffi, 2007; Youseffi *et al.*, 2006). In the 2xxx series alloy, the volume of liquid phase is slightly increased by adding silicon in small amount causing the improvement of tensile strength (Schaffer, 2004). However, pressureless sintering of pure aluminium with high content of silicon was found to be unfeasible to obtain high sintered density. Alternative process, such as hot pressing was applied to achieve high density (Yilmaz and Altintas, 1996).

2.3.2 The Effects of Compaction Pressures

As described in section 2.2.2.2 that applying high compaction pressure can disrupt the oxide layers through the plastic deformation of aluminium powder resulting in cracks occurred at the point where the powders touch each another. This can be explained by the compaction phenomenon (German, 1994) that the powder initially has the density approximately equal to the apparent density after die filling. Applying initial pressure causes rearrangement of the powders to fill the large pore giving a higher packing density. Increasing pressure provides better packing and leads to decrease porosity with the formation of new particle contacts. The contact points then undergo elastic deformation. Higher pressures increase the density by contact enlargement through plastic deformation. However, increasing higher pressure, the density is not increased significantly due to the entire powders become work hardened. Therefore, the change in density as a function of compaction pressure can be illustrated in Figure 2.5.

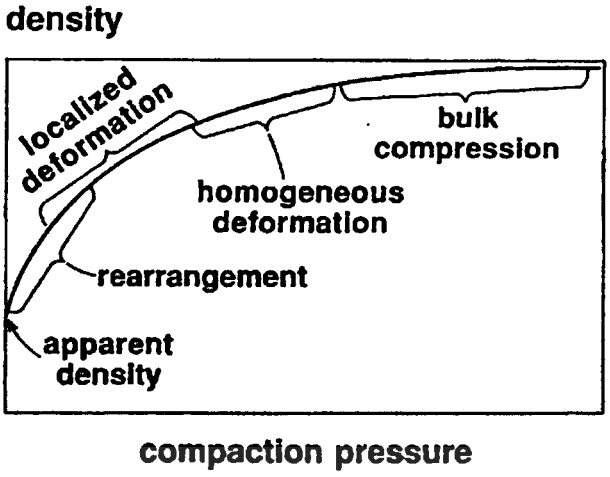

Figure 2.5 A sketch of the density versus compaction pressure during compaction of metal powder, showing key stages and declining compressibility as the density increases (German, 1994).

Gutin *et al.* (1972) investigated the effects of compaction pressure on the sintered properties, i.e. strength and relative electrical conductivity, of both lightly and severely oxidised aluminium powders compact. For the lightly oxidised aluminium powder, Figure 2.6 (a), shows that with increasing compaction pressure, the strength of the sintered specimens increased, while their electrical conductivity gradually increased and nearly approached that of the bulk aluminium specimen. In the case of severely oxidised aluminium powder, as shown in Figure 2.6 (b), the trend of the result is similar to that of Figure 2.6 (a) but there was less variation of both strength and relative electrical conductivity obtained from sintered specimens comparing with their green specimens. However, this shows the evidence that the applying high compaction pressure was more effective for the lightly oxidised powders because the oxide films were disintegrated into small fragment, enabling large contact area to be formed. For the severely oxidised powders, applying high compaction pressure was not as effective, but the additional application of the shear force helped to intensify film rupture, enabling some contact area appeared (Andreeva and Rastrigina, 1965).

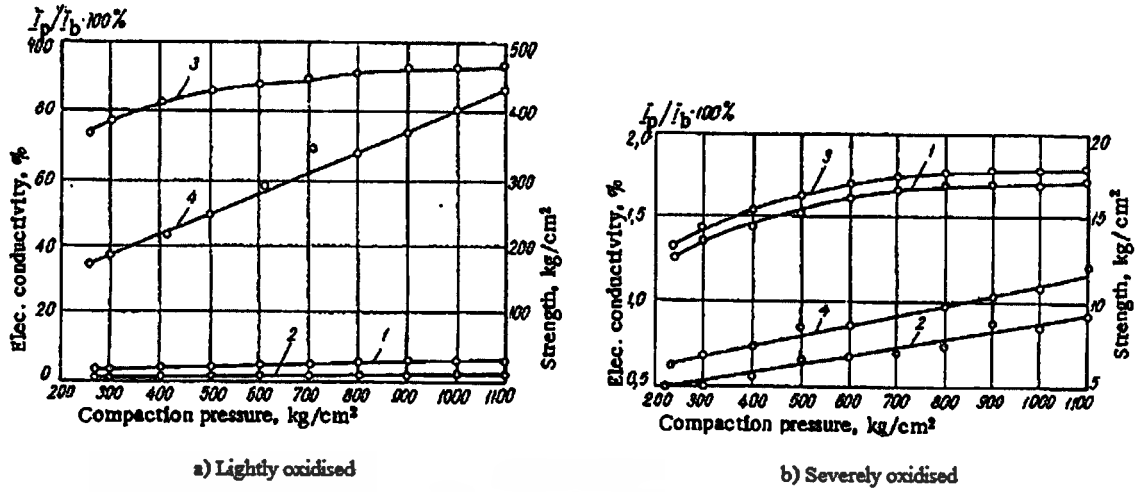

Figure 2.6 Effects of compaction pressures on the strength and relative electrical conductivity of both green and sintered specimens of (a) lightly oxidised and (b) severely oxidised aluminium powder, whereas 1 and 3 represent the green and sintered electrical conductivities and 2 and 4 represent the green and sintered strength respectively (Gutin *et al.*, 1972)

2.3.3 The Effects of Sintering Atmosphere

Sintering atmosphere is an important factor that plays a significant role during sintering, especially for aluminium, because it must act as an oxidising protector and/or partial reducing agent. Sintering atmospheres, that commonly used in aluminium sintering process, include nitrogen, argon, vacuum and mixture of nitrogen and hydrogen gases (Schaffer *et al.*, 2006). Among these four atmospheres, it has been found that nitrogen is the most effective (Pieczonka *et al.*, 2007; Schaffer and Hall, 2002; Schaffer *et al.*, 2006). Figure 2.7 shows the effects of sintering atmosphere on the densification of Al-3.8Cu-1Mg-0.7Si. The zeroth minute corresponds to the time at which the sintering temperature was first attained. Samples expanded initially under all atmospheres and then shrink over time, except where hydrogen was added to the gas stream, when no shrinkage occurred. With the other three atmospheres, the shrinkage rate was the same for the first 10 minutes, but it slowed down thereafter in argon and accelerated under nitrogen. Therefore, it showed that the efficiency of the sintering atmosphere decreased in the order: nitrogen > vacuum > argon > the mixture of nitrogen and hydrogen gases (Schaffer *et al.*, 2006). Nitrogen is effective for not only aluminium alloy but also pure aluminium as investigated by Pieczonka *et al.* (2007).

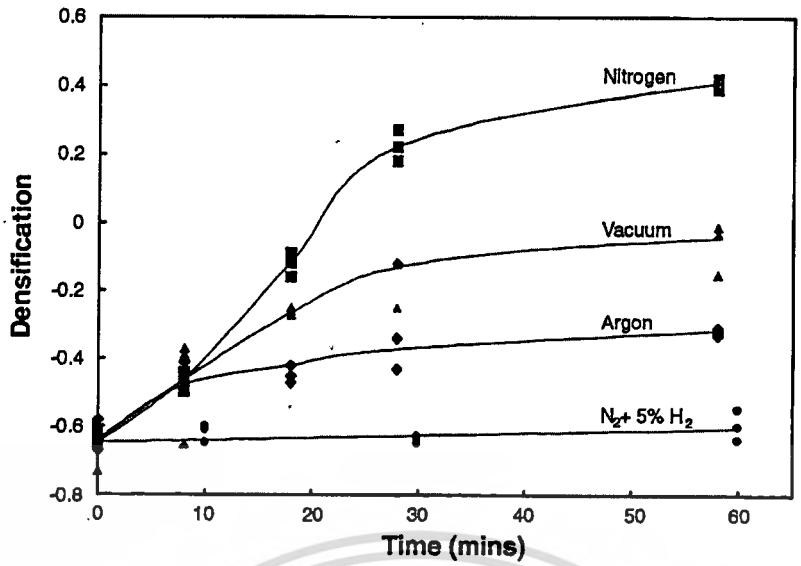

Figure 2.7 The densification of Al–3.8Cu–1Mg–0.7Si as a function of time and atmosphere (Schaffer *et al.*, 2006).

Nitrogen is not only the protective atmosphere during sintering but also acts as the reducing agent, while the others act as only the protective atmosphere. It is suggested that there is the formation of aluminium nitride (AlN) occurred when aluminium is sintered in nitrogen (Schaffer and Hall, 2002; Schaffer *et al.*, 2006). This formation comes from two reactions; the first comes from the partial reduction of Al_2O_3 by the reaction:

$$2Al_2O_3 + 2N_2 \rightarrow 4AlN + 3O_2 \tag{2.9}$$

and/or the second is the direct reaction with nitrogen according to:

$$2Al + N_2 \rightarrow 2AlN \tag{2.10}$$

However, these reactions can only occur if the partial pressure of oxygen is below the critical value, P_C, which is given by:

$$P_C = \left[P_{N_2} \frac{a_{Al_2O_3}}{a_{AlN}^2} e^{\left(\frac{-\Delta G}{RT}\right)} \right]^{2/3} \tag{2.11}$$

where P_{N_2} is the partial pressure of nitrogen, $a_{Al_2O_3}$ and a_{AlN} the activities of Al_2O_3 and AlN respectively, R the gas constant, T the temperature, and ΔG the change in free energy for the reaction. It is also found that the critical partial pressure of oxygen at 620°C is 2.56×10^{-32} Pa.

This is below the concentration of oxygen in the commercial nitrogen gas. Furthermore, it is found that the reduction by nitrogen can be occurred through the self-gettering phenomenon (Schaffer and Hall, 2002).

Self-gettering phenomenon can be explained that as the temperature increases, the oxide layer grows. This will decrease the oxygen partial pressure in the gas as it travels into the pore network. The fresh gas impinging on the surface of the compact will have a high oxygen partial pressure. However, deep in pore network, where the gas flow rate is much lower than on the surface, the oxygen may be consumed by aluminium faster than it can be replenished by the incoming gas. The local oxygen partial pressure will then fall. Therefore, this suggests that the sample surface will have less sinterability because it is always exposed to oxygen of the impinging gas. While the core of specimen will sinter more readily because the oxygen partial pressure is relatively low and induced the partial reduction via nitrogen. The result of this effect can be observed as illustrated in Figure 2.8 that there is an unsintered layer near the sample surface and well sintering is observed at the core of sample (Schaffer and Hall, 2002).

Figure 2.8 The optical microstructure through the cross section of an Al-0.1Mg sample sintered in nitrogen. The outer surface was unsintered aluminium but inner core showed well sintering and consisted of both Al (grey) and AlN (white) phases (Schaffer and Hall, 2002).

In addition to the sintering atmosphere, another oxidising agent during sintering of aluminium is the water vapour or moisture. The relevant parameter of the water vapour is known

as dew point. The dew point is the temperature at which the water vapour will condense and it is used to indicate the level of water vapour content in the atmosphere (Lutgens and Tarbuck, 1998). Ideally, the required atmosphere dew point in order to completely reduce aluminium oxide is -140°C at sintering temperature of 600°C (Lumley *et al.*, 1999), which is difficult to reach. In practice, a dew point of -40°C is rather arbitrarily defined as the maximum allowable water level (Dudas and Dean, 1969). Higher level of moisture is detrimental to the properties as shown in Figure 2.9. The sintering response of Al-3.8Cu-1Mg-0.7Si is retarded at dew point more than -60°C. However, for dew point higher than -60°C, the powder compact showed less densification and was begun to expand (Scahffer *et al.*, 2006). This is suggested that the water vapour acts as the stabiliser of aluminium oxide, which hinders shrinkage due to one of the stable phases of aluminium oxide is the hydrated aluminium oxide (Krajnikov *et al.*, 2002; Scahffer *et al.*, 2006).

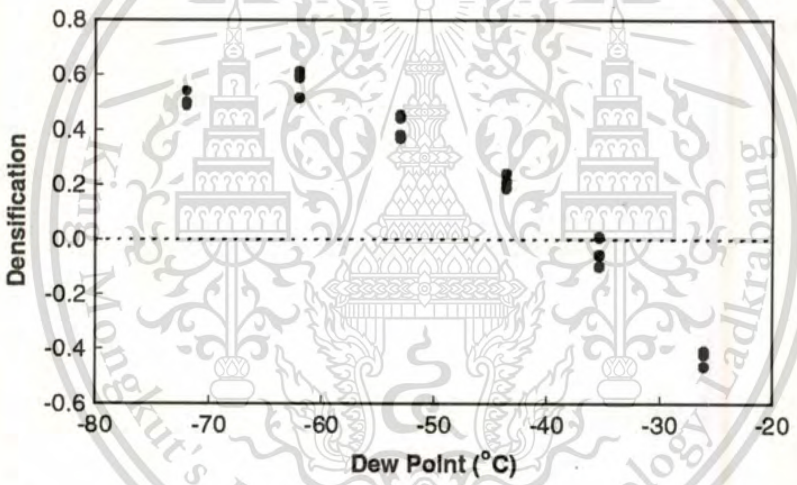

Figure 2.9 Effect of dew point of nitrogen on the densification of Al–3.8Cu–1Mg–0.7Si, pressed at 100 MPa and sintered for 30 minutes (Schaffer *et al.*, 2006).

2.4 Development of High Wear Resistant Aluminium Based Alloy Through P/M Process

P/M aluminium alloys have high potential in automotive components, particularly for sliding and friction parts. Most of the structural P/M aluminium alloys used today are based on wrought or cast alloy compositions, for example, the 2xxx and 6xxx alloy series that contain copper, magnesium and/or silicon (Schaffer, 2004). However, their low wear resistance comparing to other materials, limits their applications.

Cast aluminium-silicon (Al-Si) alloys are a common choice for such application. The alloys with an average silicon content ranging from 10% wt.-17% wt., have coarse silicon crystals growing during solidification. Higher silicon content was also found to increase the wear resistance and thermostability (Vukcevic and Delijic, 2002). However, P/M processing offers some significant advantages over casting, particular in its ability to produce an alloy with relatively fine silicon particles, which results in the better wear resistant products.

Recently, there have been works on the vacuum sintering of hypereutectic P/M Al-Si alloys by conventional P/M process (Yilmaz and Altintas, 1996). They were found to be unfeasible in terms of obtaining high sintered density. Therefore, an alternative process, for example, hot pressing had to be carried out in order to improve such properties (Yilmaz and Altintas, 1996). However, the addition of pre-alloyed or master alloyed powder of Al-Si alloy into the elemental powder can improve both physical and mechanical properties through the conventional P/M process (LaDelpha *et al.*, 2008). This is due to the fine structure within the atomised master alloy is retained and overall refinement of the silicon crystals is ensued after sintering. While the elemental addition of silicon particles yielded relatively coarse silicon crystals in the sintered products and the poor dispersion of silicon crystals as compared with those achieved by master alloy addition.

Another development of P/M Al-Si alloy is by Neubing *et al.* (2002). Their development was also based on the powder mixture of pure aluminium and a master alloy containing the alloying elements. The nominal compositions of this alloy consisted of Al-14Si-2.5Cu-0.6Mg. Sintering process was carried out in dry nitrogen with the dew point of less than -45°C and at the sintering temperature of 555°C for 60 minutes, the tensile strength of 230 MPa with the elongation of 1.4% and the Brinell hardness of 105 HB were obtained. By using this alloy and sintering parameters, Casella *et al.* (2004) investigated that this P/M aluminium alloy exhibited good wear resistance similar to that obtained by casting. The mainly reason was due to a good sinterability between powders, which can be seen from the microstructure in Figure 2.10. It shows a duplex microstructure resulting from the intermixing of aluminium matrix and master alloy and dispersion of the fine hard phase of silicon in the aluminium matrix.

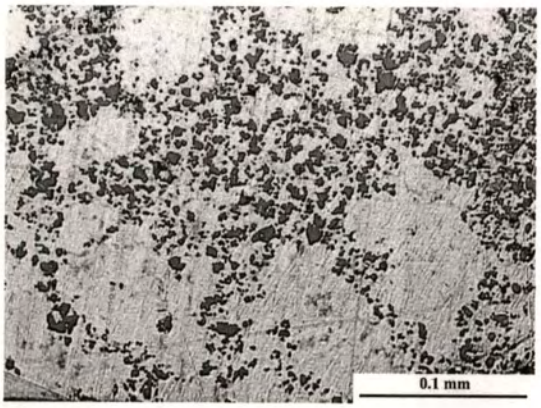

Figure 2.10 Microstructure of the P/M Al-Si alloy observed by Casella *et al.* (2004).

CHAPTER 3

EXPERIMENTAL PROCEDURES

3.1 Material

The aluminium alloy powder used in this study was the air-atomised aluminium-silicon-copper-magnesium (Al-Si-Cu-Mg) alloy. Its commercial name is Alumix 231, supplied by ECKA Granulate, GmbH, Germany. The chemical compositions and powder size distribution are shown in Table 3.1. High percentage of silicon (14.9% wt.) was added to increase the wear resistance. It is noted that 1.5% by weight of Ethylene-bis-stearamide wax was admixed with the powder as lubricant. The powder had a wide size distribution from smaller than 45 μm to up to 250 μm. However, the majority of powder (50% wt.) lied within 45-100 μm range. This can be supported by the scanning electron image of this powder in Figure 3.1. The shape of the powder was irregular and the powders were clustered together by the admixed wax as visible in circles. It was found by Neubing *et al.* (2002) that the powder used in this work was the mixture of pure aluminium powder and the master alloy powder of Al-Si-Cu-Mg.

Table 3.1 Chemical compositions and powder size distribution of aluminium alloy used in this study (From: certification of inspection No. EN 10204, ECKA Granulate, GmbH).

Chemical composition							
Element	Aluminium	Silicon	Copper	Magnesium	Lubricant		
Weight (%)	Balanced	14.9	2.4	0.55	1.5		
Powder size distribution							
Size range (μm)	<45	45-63	63-100	100-160	160-200	200-250	>250
Weight (%)	35.6	24.9	25.3	12.0	1.7	0.5	0.0

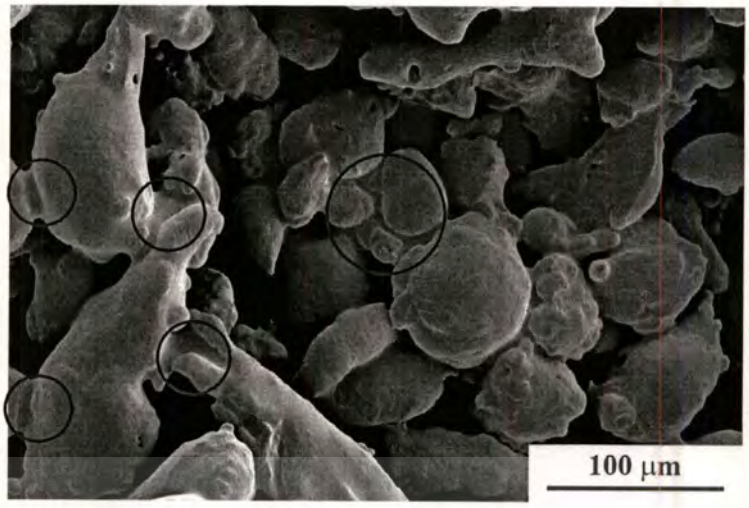

Figure 3.1 Scanning electron micrograph of the aluminium alloy used in this study. The circles show the powders clustered together by the admixed wax.

3.2 Experimental Procedures

3.2.1 Introduction

The overall experimental procedures in this work were based on the conventional P/M process shown as a flow chart in Figure 3.2. Initially, the aluminium alloy powder was compacted into tensile specimens by a pressing machine. The compacted specimens were commonly called "green specimens". Subsequently, the green specimens were dewaxed and sintered by using the recommended parameters (ECKA Granulate GmbH, 2007) as shown in Table 3.2. These parameters can be performed as the thermal cycle shown in Figure 3.3, which is a three step operation consisting of dewaxing, sintering, and cooling. Initial operation was the dewaxing step, in which the temperature was raised from the room temperature to the dewaxing temperature of 420°C with the heating rate of 5°C/min. This temperature was then hold for 60 minutes to ensure that the lubricant was completely removed before continuing to the sintering step. The sintering step was then started by raising temperature from dewaxing temperature to the sintering temperature of 560°C with the heating rate of 5°C/min. The holding step was also applied in the sintering step for 60 minutes. The final step was cooling, in which the heating was stopped and the sintered compacts were allowed to be cooled down to the room temperature within the sintering gas in the furnace.

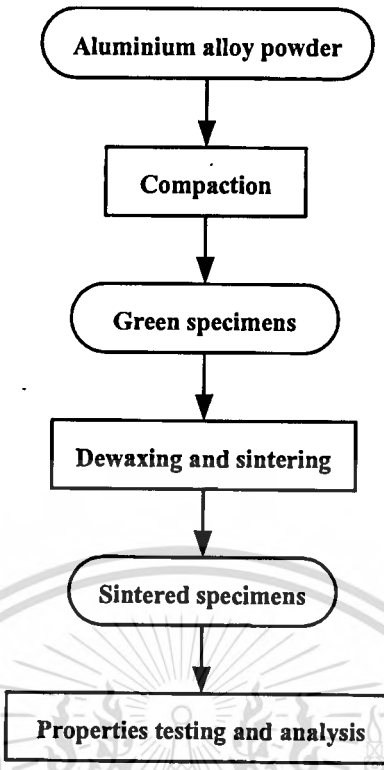

Figure 3.2 Flow chart of the conventional powder metallurgical (P/M) process.

Table 3.2 The recommended sintering parameters (ECKA Granulate GmbH, 2007).

Dewaxing temperature (°C)	380-420, or direct at sintering temperature
Sintering temperature (°C)	550-560
Sintering time (Minutes)	60
Sintering atmosphere	Nitrogen

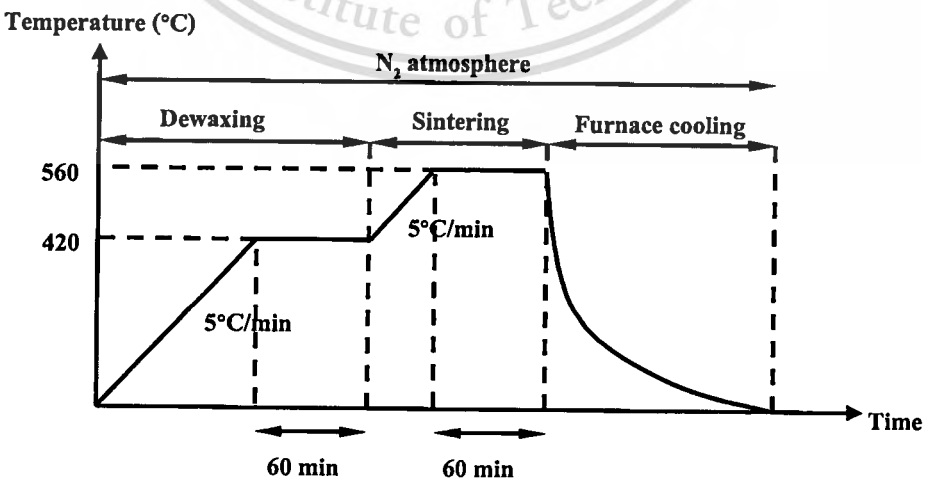

Figure 3.3 Thermal cycle for sintering.

In this work, there were two main parameters that were studied, namely sintering condition and compaction pressure. In order to evaluate the effects of these two parameters, the properties of the sintered specimens both the physical and mechanical properties, which are density, shrinkage, microstructure, oxygen contents, tensile test and hardness test, were examined and discussed. The methodology to examine the properties of the specimens is explained in detail later.

3.2.2 The Effects of Sintering Conditions

In this part, the aluminium alloy powder was initially compacted into tensile specimens with the green density of 2.50±0.01 g/cm^3 or 93.6±0.4% theoretical density (% TD) (ECKA Granulate GmbH, 2007). It is noted that the theoretical density of this material was 2.67 g/cm^3. For sintering, there were four sintering conditions designated as conditions *A, B, C,* and *D,* in which there were several items to be adjusted for each condition such as the level of vacuum applied before starting the thermal cycle, control atmosphere, the purity of nitrogen gas, the chamber type and capacity. The details of each condition can be summarised in

Table 3.3. Initially, to compare the effects of sintering gas, nitrogen gas with different purity, which were 99.99% and 99.999%, was used in conditions *A* and *B* respectively. To reduce the oxygen and contamination in the furnace, the low and high level of vacuum were applied for comparison between conditions *B* and *C*. Lastly, the effect of control atmosphere was carried out for comparison between conditions *C* and *D* by changing the control atmosphere from pressure controlling to flow controlling. However, the sintering parameters were still referred to the recommendation in Table 3.2.

Table 3.3 The variation of sintering conditions.

Conditions	Level of vacuum applied before heating	Control atmospheric	Purity of nitrogen gas (%)	Nitrogen flow rate (l/min)	Sintering chamber	Chamber capacity (liters)
A	Low*	Pressure	99.99	6	Graphite box	165
B	Low*	Pressure	99.999			
C	High**	Pressure	99.999			
D	N/A	Flow	99.999	4	Ceramic tube	5.3

Note: *Low = low level of vacuum of 2×10^{2} Pa was applied before starting the thermal cycle.

**High = high level of vacuum of 1×10^{-3} Pa was applied before starting the thermal cycle.

The experimental results were separated into two sections, firstly, the results of atmosphere dew point affected by sintering conditions and secondly, the effects of sintering conditions on sinterability of aluminium alloy.

3.2.3 The Effects of Compaction Pressure

The variable in this part was the compaction pressure. The aluminium alloy powder was compacted with several compaction pressures ranging from 150-700 MPa. The green specimens were sintered by using the best condition obtained from section 3.2.2. To evaluate the effects of this parameter, the sintered properties, such as physical and mechanical properties, were measured and discussed.

3.3 Testing of Properties

3.3.1 Physical Properties

3.3.1.1 Density

The density measurement was based on the Archimedes' principle. This corresponded to the standard test method of ASTM B311 (ASTM International, 2005). The density can be calculated as follows:

$$\rho = \frac{(m_a \times \rho_w)}{(m_a - m_w)} \tag{3.1}$$

where, ρ = the density of test specimen (g/cm^3),

m_a = mass of test specimen in air (g),

m_w = mass of test specimen in water (g),

ρ_w = the density of water at the measuring temperature (g/cm^3).

The green density was not measured for all specimens due to the reaction of aluminium with water. Water submersion could cause the water to remain within the pore and then could deteriorate the sinterability of aluminium powders. Therefore, only the green

density of one specimen from every five pieces was measured. It is possible to control the deviation of density to be ±0.01 g/cm^3. However, the sintered density was measured for all specimens.

3.3.1.2 Dimensional Change

The dimensional change of the sintered specimens was measured relatively to their green specimens. The measurement was taken at five specific positions as shown in Figure 3.4 and each position was designated as W_1, W_2, W_3, L, and T.

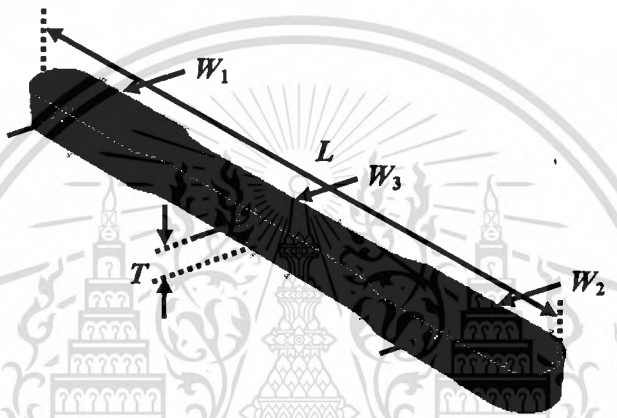

Figure 3.4 The specific positions for measuring dimension in the specimen.

The dimensional change (DC) of the sintered specimens from their green stage can be calculated as follows:

$$DC = \frac{(D_g - D_s)}{D_g} \times 100 \qquad (3.2)$$

where, DC = the dimensional change in which the positive sign indicates shrinkage, while the negative sign indicates expansion (%),

D_g = the dimension at a specific position of the green specimen (mm),

D_s = the dimension at a specific position of the sintered specimen (mm).

3.3.1.3 Oxide Analysis

Takahashi (2008) suggested a technique to determine the oxide contents by using the scanning electron microscope (SEM) equipped with the energy dispersive

spectroscopy (EDS). By this technique, the unknown oxygen contents in the aluminium alloy specimen were measured relatively to the aluminium oxide or alumina (Al_2O_3). The calculation of the oxide content can be explained as follows:

Considering the electron beam with intensity, I, projected on alumina (Al_2O_3) specimen, the percentage by weight of aluminium detected by EDS, $W_{Al(Al_2O_3)}$ can be represented as a function of beam intensity as follows,

$$W_{Al(Al_2O_3)} = \frac{2}{5} k_{Al} I \tag{3.3}$$

where, $W_{Al(Al_2O_3)}$ = the percentage by weight of aluminium in Al_2O_3 detected by EDS (% wt.),

k_{Al} = the proportional constant for aluminium,

I = the intensity of electron beam,

and number $\frac{2}{5}$ is the ratio of 2 aluminium atoms from 5 atoms of Al and O in alumina (Al_2O_3).

The percentage by weight of oxygen detected by EDS, $W_{O(Al_2O_3)}$, can also be represented as a function of beam intensity in a similar way as follows,

$$W_{O(Al_2O_3)} = \frac{3}{5} k_O I \tag{3.4}$$

where, $W_{O(Al_2O_3)}$ = the percentage by weight of oxygen in Al_2O_3 detected by EDS (% wt.),

k_O = the proportional constant for oxygen,

and number $\frac{3}{5}$ is the ratio of 3 oxygen atoms from 5 atoms of Al and O in alumina (Al_2O_3).

Dividing Equation (3.4) by Equation (3.3) yields,

$$\frac{W_{O(Al_2O_3)}}{W_{Al(Al_2O_3)}} = \frac{3}{2} \frac{k_O}{k_{Al}} \tag{3.5}$$

Then, the electron beam with the same intensity projected on the aluminium alloy specimen with unknown oxide content was considered. It is noted that the intensity should be equal if the same accelerating voltage is used. If x is the unknown value of oxygen content relative to aluminium content in an aluminium alloy sample, the ratio of oxygen to aluminium in the aluminium alloy specimen can be written as O : Al = x : 1. By using the

same relation as Equations (3.3) and (3.4), the percentage by weight of aluminium, $W_{Al(Sample)}$, and oxygen, $W_{O(Sample)}$, detected by EDS can be represented as a function of beam intensity as follows,

$$W_{Al(Sample)} = \left(\frac{1}{1+x}\right) k_{Al} I \tag{3.6}$$

$$W_{O(Sample)} = \left(\frac{x}{1+x}\right) k_O I \tag{3.7}$$

where, $W_{Al(Sample)}$ = the percentage by weight of aluminium in aluminium alloy sample detected by EDS (% wt.),

$W_{O(Sample)}$ = the percentage by weight of oxygen in aluminium alloy sample detected by EDS (% wt.).

Dividing Equation (3.7) by Equation (3.6) yields,

$$\frac{W_{O(Sample)}}{W_{Al(Sample)}} = \frac{x}{1}\frac{k_O}{k_{Al}} \tag{3.8}$$

Substituting of $\frac{k_O}{k_{Al}}$ from Equation (3.5) into Equation (3.8) yields,

$$\frac{W_{O(Sample)}}{W_{Al(Sample)}} = \frac{x}{1} \cdot \frac{2}{3}\frac{W_{O(Al_2O_3)}}{W_{Al(Al_2O_3)}} \tag{3.9}$$

Therefore, the oxygen per aluminium contents value, x, can be calculated from the following equation,

$$x = \frac{3}{2} \cdot \frac{W_{Al(Al_2O_3)}}{W_{O(Al_2O_3)}} \cdot \frac{W_{O(Sample)}}{W_{Al(Sample)}} \tag{3.10}$$

3.3.1.4 Microstructure Preparation

The method to prepare specimens for microstructural observation started from the sintered specimen was cut into a small piece to reveal the cross section. The specimen was then hot mounted in the epoxy resin. To reveal the clear and smooth microstructure, the specimen was firstly ground by the silica papers and subsequently fine polished with the diamond suspension. The steps of the grinding and fine polishing (ASM International, 2004) were tabulated in Table 3.4.

Table 3.4 Grinding and fine polishing for aluminium P/M specimens (ASM International, 2004).

Grinding					
Step	**Abrasive**	**Grade**	**Lubricant**	**Rotating speed (rpm)**	**Time (minute)**
1	SiC	500	H_2O	200	1-5
2	SiC	1000	H_2O	200	1
3	SiC	2400	H_2O	200	2.5

Fine polishing						
Step	**Cloth**	**Abrasive**	**Gradation**	**Lubricant**	**Rotating speed (rpm)**	**Time (minute)**
1	Nap	D.P.*	3 μm	Alcohol based	150	1**
2	Nap	D.P.*	1 μm	Alcohol based	150	1.5***

Note: * D.P. = diamond paste.

** If there were still scratches remaining from grinding step, the 1st step of fine polishing should be continued.

*** If there were still scratches appeared on the specimen, the 2nd step of fine polishing should be continued until the scratches were eliminated.

3.3.2 Mechanical Properties

3.3.2.1 Macro Hardness

The Rockwell scale F or HRF hardness test was selected to measure the apparent macroscopic hardness of the specimen. The test was carried out by indenting the 1/16" steel ball with the applied load of 60 kgf for 6 seconds according to the standard test method MPIF standard number 43 (Metal Powder Industries Federation, 2002). Two of eight specimens were selected to test and the total test point was eight.

3.3.2.2 Tensile Properties

The other five pieces of sintered specimens were selected to test their tensile properties including ultimate tensile strength and elongation according to the standard test method for determination of tensile properties of the P/M materials, MPIF standard number 10 (Metal Powder Industries Federation, 2002).

CHAPTER 4

THE EFFECTS OF SINTERING CONDITIONS ON PROCESS ABILITY OF Al-Si-Cu-Mg ALLOY

4.1 Effects of Sintering Conditions on Atmosphere Dew Point

Table 4.1 shows the atmosphere dew point affected by sintering conditions as shown in Table 3.3. Dew point temperature is the temperature at which the water vapour in the atmosphere will condense (Lutgens and Tarbuck, 1998). It also indicates the level of moisture in the atmosphere in which the lower dew point temperature indicates the lower level of moisture in the atmosphere.

Table 4.1 Atmosphere dew point affected by the sintering conditions.

Conditions	Level of vacuum applied before heating cycle	Control atmosphere	Purity of nitrogen gas (%)	Nitrogen flow rate (l/min)	Sintering chamber	Chamber capacity (liters)	Dew point (°C)
A	Low	Pressure	99.99	6	Graphite box	165	-29.4
B	Low	Pressure	99.999				-31.7
C	High	Pressure	99.999				-33.1
D	N/A	Flow	99.999	4	Ceramic tube	5.3	-38.4

From the results of atmosphere dew point obtained from various sintering conditions as shown in Table 4.1, it is apparent that the purity of nitrogen gas affected directly the atmosphere dew point. By using higher purity of nitrogen gas in sintering condition *B* (99.999%) comparing with sintering condition *A* (99.99%), lower dew point temperature was obtained because of the higher purity of gas, the less moisture content.

By applying high vacuum level before heating in sintering condition *C* slightly decreased the atmosphere dew point comparing with sintering condition *B*. The slightly decrease was because the initial applying of higher level of vacuum evacuated more impurities including moisture than lower level of vacuum while the other parameters were similarly during sintering. However, it is found that the dew point temperature was significantly improved by using the ceramic-tube furnace with the permanent flowing of nitrogen gas as shown in condition *D*.

The results also show that sintering in flow controlling atmosphere gave lower dew point temperature than pressure controlling atmosphere because the water vapour in the atmosphere was continuously swept out by permanent flowing of gas. In contrast, for pressure controlling atmosphere, the pressure of the sintering atmosphere was always kept to be constant. Therefore, the rate of sweeping out of water vapour was less, although the gas flow rate is lower in condition *D*.

In conventional P/M for aluminium alloy, flow controlling atmosphere is commonly used in order to produce the atmosphere with very low dew point. Moreover, not only the permanent flow of dry nitrogen gas that is necessary in order to achieve the low atmosphere dew point, the capacity of sintering chamber and the nitrogen flow rate are also crucial. It is suggested that for the furnace with the 42.5-litre chamber, the suitable gas flow rate in order to maintain a -40 to -50 °C furnace atmosphere dew point, should be 28-47 l/min (ASM International, 1984).

However, it does not mean that the graphite box furnace could not reach the low atmosphere dew point. It would be possible if the atmosphere controlling can be set as flow controlling and the gas flow rate is increased but there was the restriction of the furnace equipments that limited the operation of flow controlling using high flow rate of sintering gas.

4.2 Effects of Sintering Conditions on Physical Properties

4.2.1 Density

The sintered density of the specimens sintered in various sintering conditions comparing with their green density is shown in Figure 4.1. Initially, the average green density of all specimens was 2.50 g/cm^3 or 93.6% theoretical density (% TD). The sintered density of 98.5% TD was observed on the specimens sintered in condition *D* that had the lowest dew point. While the specimens sintered at the higher atmosphere dew points, as in conditions *B* and *C*, had sintered density of 95.5% and 95.9% TD respectively. Furthermore, the lowest sintered density of 94.0% TD was observed on the specimens sintered in condition *A* which had the highest

atmosphere dew point. Nevertheless, the specimens sintered in all sintering conditions showed the increase in density relative to their green density, which was 93.6% TD.

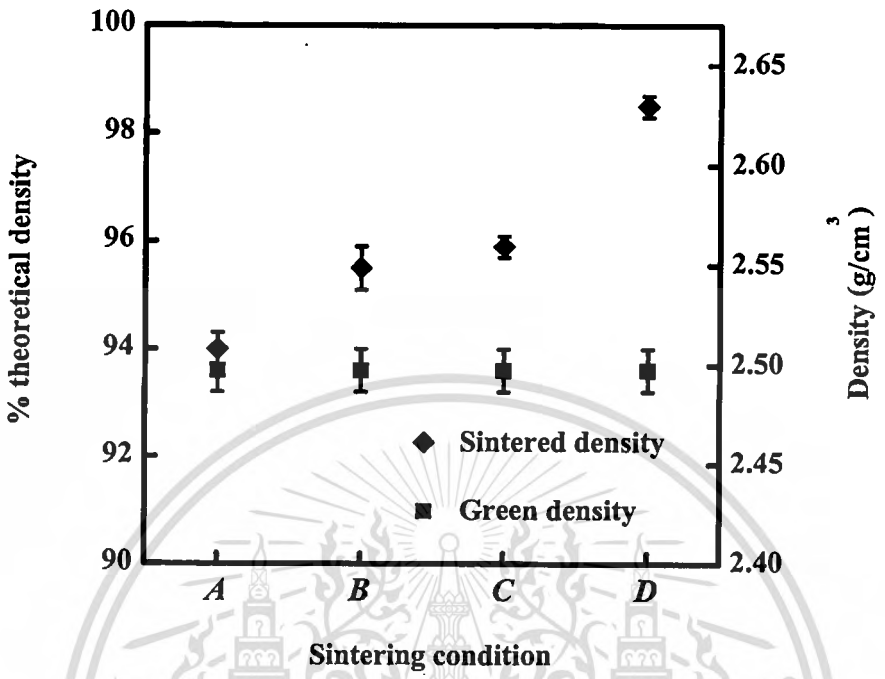

Figure 4.1 Density of the specimens sintered in different conditions.

The atmosphere dew point observed from various sintering conditions as listed in Table 4.1, it shows that sintering conditions affected directly the atmosphere dew point. The green specimens that were sintered by using different sintering conditions were also different. Therefore, the relationship between the atmosphere dew point and the sintered density can be plotted as shown in Figure 4.2. It is noted that the result obtained by Neubing *et al.* (2002) was also added into the graph for comparison. It is found that as the atmosphere dew point decreased, the sintered density increased linearly for the atmosphere dew point from -29.4°C to -38.4°C. Further decreasing dew point to -45°C, less significant increasing of density was observed. This suggested that the densification was nearly reached saturation, which meant that the sintered density would be constant even the dew point was decreased further (Schaffer *et al.*, 2006).

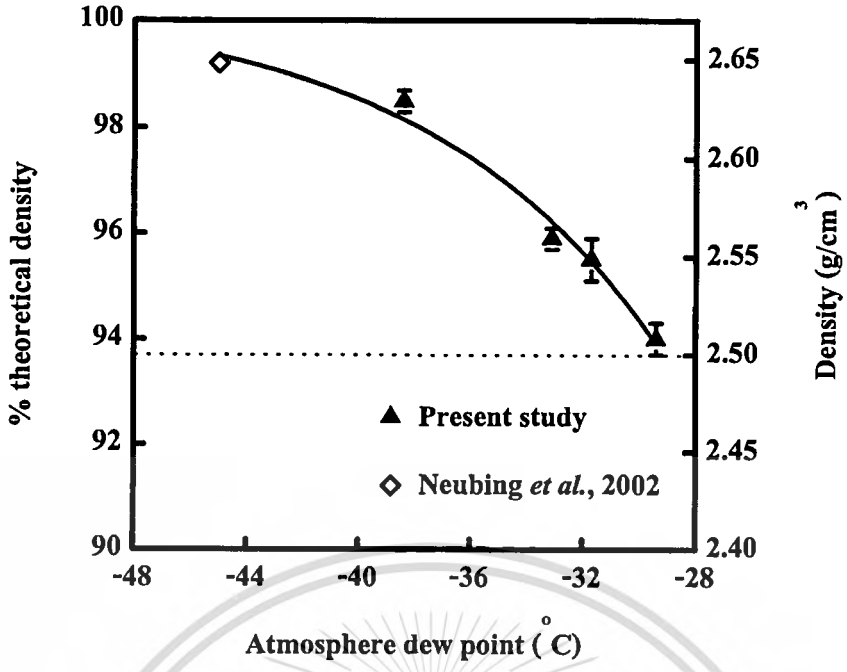

Figure 4.2 Sintered density of the specimens as a function of atmosphere dew point.

4.2.2 Dimensional Change

From the previous section, there was the increase in sintered density relative to green density. This had to be accompanied by the shrinkage of the specimens. The linear shrinkage at a specific position of specimens sintered in each sintering condition was shown in Figure 4.3. The result showed that the largest shrinkage occurred on the specimens sintered in condition *D* at every position and the shrinkage was decreased for conditions *C*, *B*, and *A* respectively. This is in good agreement with the sintered density shown in Figure 4.1. The shrinkage at position W_1, W_2, W_3, were nearly the same as shown in Figure 4.3 (a). Hence, the average of these three positions was then calculated as shown in Figure 4.3 (b). In addition, it was observed that the shrinkage in the direction perpendicular to the pressing direction, which were W_1, W_2, W_3 and the shrinkage for *L*, was similar as shown in Figure 4.3 (c). While the direction parallel to the pressing direction (*T*), the shrinkage was significantly less as shown in Figure 4.3 (d). Moreover, there was nearly zero shrinkage at position *T* observed on the specimens sintered in condition *A*.

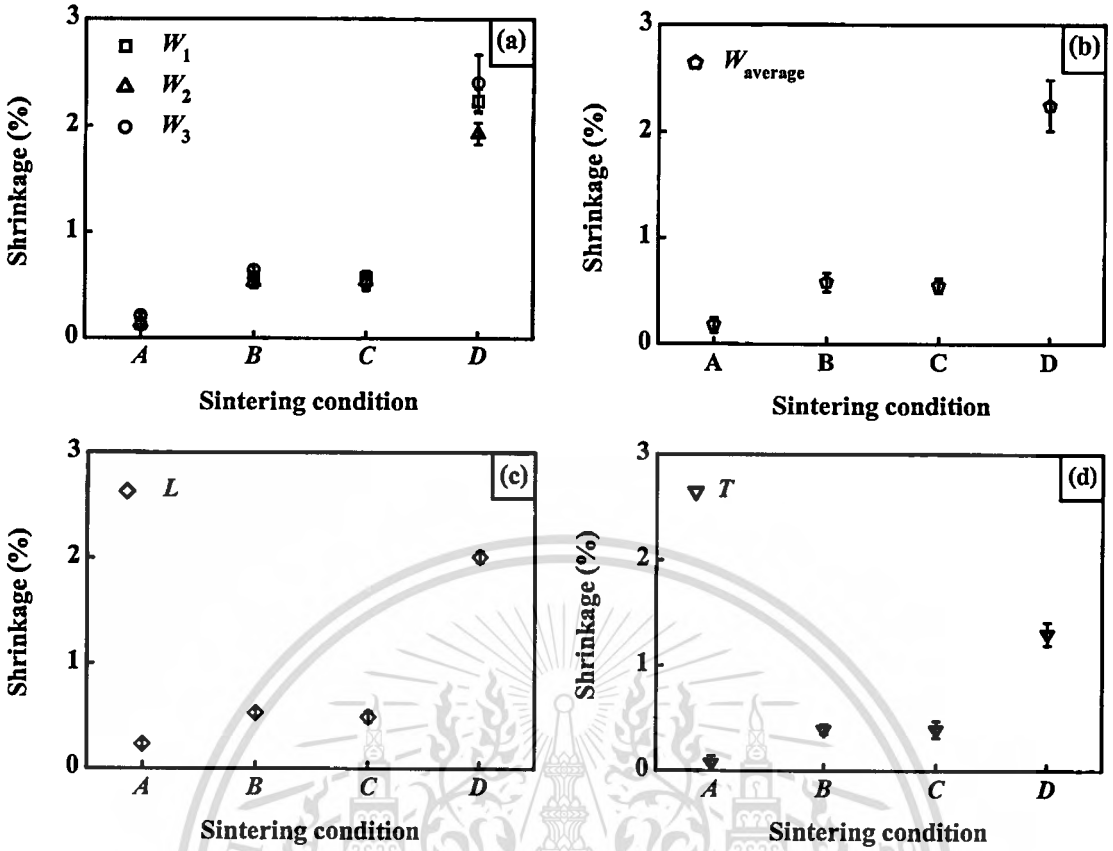

Figure 4.3 The linear shrinkage of the specimens at specific positions for each sintering condition, (a) W_1, W_2, W_3, (b) $W_{average}$, (c) L, (d) T.

Although the linear shrinkage at the specific position shows the result corresponding to the density and the atmosphere dew point, there was the non-uniform shrinkage between the directions perpendicular and parallel to the pressing direction observed at all specimens. It was resulted from the density gradient within the compacted specimens that usually occurred in the uniaxial compaction (German, 1994). The powders were more densified along with the pressing direction than those along the perpendicular to the pressing direction because the powders were subjected directly to the applied load. In addition, the uniaxial compaction caused the powders to elongate perpendicular to the pressing direction and consequently the pores trended to be elongated in perpendicular to pressing direction. However, the pores trend to spheroidise during sintering, this will cause the more shrinkage in the direction perpendicular to the pressing direction and less shrinkage in the parallel pressing direction (German, 1996).

Both density and shrinkage indicated that atmosphere dew point affected the densification of the powder, but how was still remain as the question. Therefore, microstructural

study was another way to explain what happened during sintering in different atmosphere dew points.

4.2.3 Microstructures

The microstructures of the green specimens are shown in Figure 4.4. It shows that the Al-Si-Cu-Mg alloy powder used in this study is the mixture of the aluminium powder with the master alloy of Al-Si-Cu-Mg. After compaction, the softer aluminium powder was deformed by the harder master alloy and hence, the greater contact areas were generated between those two types of powders or between themselves. The pores were irregular and some pores were flattened. This microstructure was similar to that observed by Neubing *et al.* (2002).

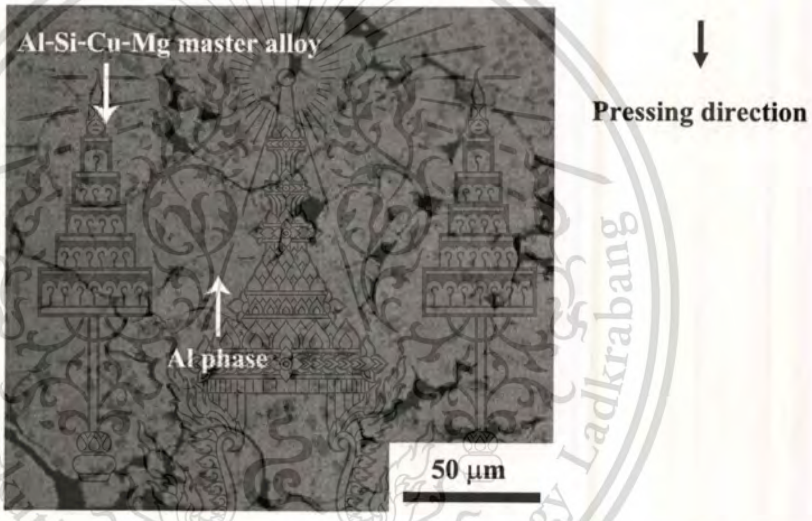

Figure 4.4 Microstructural image of the green specimen compacted at 700 MPa. It is noted that the pressing direction is vertical.

Figure 4.5 shows the microstructures of the specimen sintered in different conditions. All microstructures exhibited the dispersion of silicon phase in the aluminium matrix. However, the homogeneity of silicon phase dispersion was varied with the sintering conditions. The microstructure of the specimen sintered in condition *A*, Figure 4.5 (a), exhibited the poorest dispersion and there were still a large number of pores distributed throughout the specimen. While the microstructure of the specimens sintered in conditions *B* and *C*, Figure 4.5 (b) and (c), exhibited more homogeneous dispersion of silicon phase, pore size and a large number of pores were reduced. Moreover, it was found that the specimen sintered in condition *D* had the most homogeneous dispersion of silicon phase with minimal porosity as shown in Figure 4.5 (d). In

addition, there were more pores distributed at the superficial region of the specimens sintered in all conditions as seen in Figure 4.5 (e)-(h) respectively. It is noted that the superficial microstructure observed for condition *A* (Figure 4.5 (e)) exhibited the similar microstructure to the centre (Figure 4.5 (a)), which consisted of pores distributed throughout the specimens.

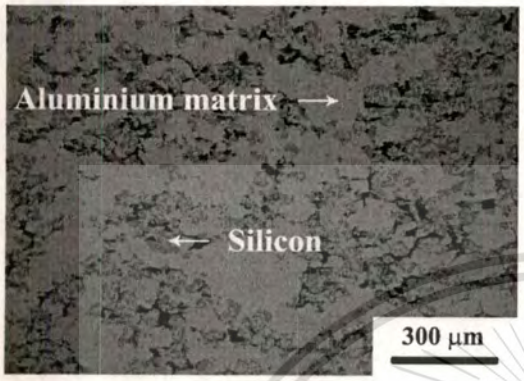

a) Condition *A* (Centre)

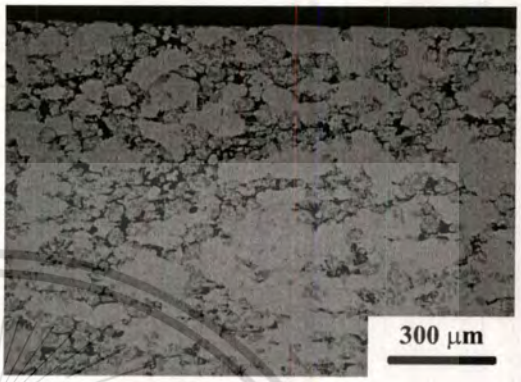

e) Condition *A* (Superficial)

(b) Condition *B* (Centre)

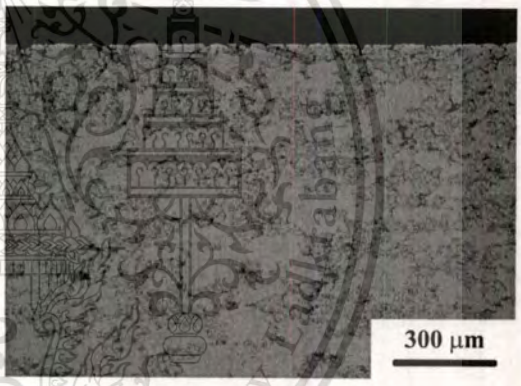

(f) Condition *B* (Superficial)

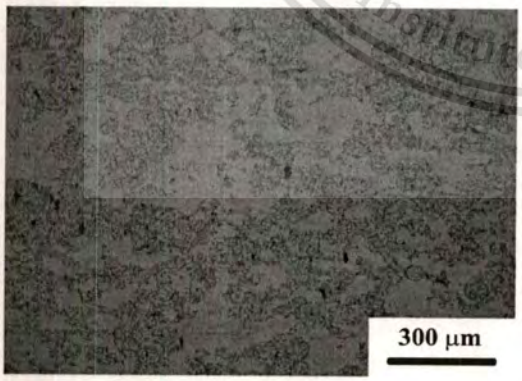

(c) Condition *C* (Centre)

(g) Condition *C* (Superficial)

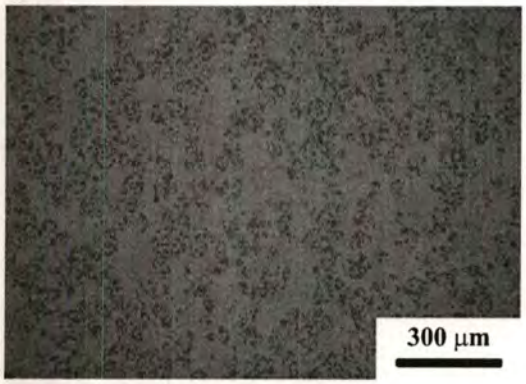

(d) Condition *D* (Centre)

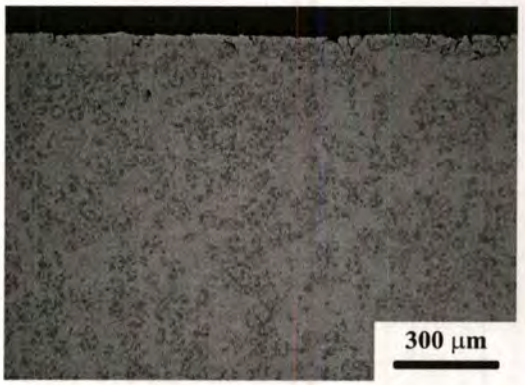

(h) Condition *D* (Superficial)

Figure 4.5 Microstructural images of the specimens sintered in (a) and (e) condition *A*, (b) and (f) condition *B*, (c) and (g) condition *C*, and (d) and (h) condition *D*. (a)-(d) were the microstuctures observed at the central regions, while (e)-(h) were those observed at superficial regions.

The microstructural results in Figure 4.5 shows that sinterability of Al-Si-Cu-Mg alloy was affected by the atmosphere dew point. If the moisture in the sintering atmosphere was high, especially in condition *A* (Figure 4.5 (a)), it was possible that the revealed fresh aluminium surface from the reduction mechanism, especially for the master alloy powders that located near the pore, could be exposed to the moisture in the sintering atmosphere. Hence, oxide was still formed again and prevented particle bonding. This could cause the pores to retain their shape without any densification. In this case, partial sintering was observed and occurred at some points of contact that was not exposed to the moisture because some oxide layers were ruptured by the applied pressure and the fresh metal was allowed to contact each other, resulting in diffusion took place at these areas during sintering (Gutin *et al.*, 1972). As the atmosphere dew point was decreased, the sinterability of aluminium alloy was improved until, shown in Figure 4.5 (b), (c) and (d). There were less pores remained in the microstructure and the dispersion of silicon phase in the aluminium matrix was more homogeneous as shown in Figure 4.5 (d).

Moreover, the microstructures observation performed in this work reveal the existence of a porous superficial region as shown in Figure 4.5 (f)-(h). This existence of a porous superficial region was in agreement with Casella *et al.* (2004), who observed an unsintered layer of aluminium-silicon alloy. It was suggested that the self-gettering phenomenon was occurred (Schaffer and Hall, 2002). By this phenomenon, the oxide layer grows as the temperature increases. This will decrease the oxygen partial pressure in the gas as it travels into the pore

network. The fresh gas impinging on the surface of the compact will have a high oxygen partial pressure. However, deep inside the pore network, where the gas flow rate is much lower, the oxygen is be consumed by aluminium faster than it can be replenished by the incoming gas. The local partial pressure oxygen will then fall. Therefore, this suggests that the specimen surface had poor sinterability because it was always exposed to oxygen in the impinging gas, while better sinterability was occurred deep inside the pore network because the oxygen partial pressure was lower.

According to the self-gettering phenomenon, it seemed to give precedence to only oxygen. However, water vapour or moisture was also the oxidising agent for aluminium and it was found that the rate of oxidation of aluminium with the moisture was faster than with the oxygen at the sintering temperature (Kim *et al.*, 1996). If the self-gettering was occurred only with oxygen, the question was why sintering condition *D* gave better sinterability at the superficial region than that observed for condition *C*. It is noted that the high vacuum was applied for the condition *C* but not for condition *D* and additionally both conditions used the same gas. Therefore, self-gettering can be occurred not only oxygen but also water vapour. If the water vapour in the atmosphere was low or low atmosphere dew point, the effects of self-gettering was less as observed in this work.

In addition, it is also suggested that nitrogen can partially reduce the oxide of aluminium to form the AlN according to equation (2.9) (Schaffer and Hall, 2002; Schaffer *et al.*, 2006). Although nitrogen atmosphere was used in the all sintering conditions but no evidence of AlN formation was occurred as shown in the energy dispersive spectrum (EDS) analysis in Figure 4.6 (a) and (b). It is noted that the EDS analysis at the centre of the specimens sintered in only conditions *C* and *D* was selected to show. There were peaks of aluminium, silicon, copper, magnesium and oxygen but there was no nitrogen peak. Hence, the partial reduction of oxide to form AlN was not achievable in this experiment. It suggested that AlN could be formed if both high vacuum and low atmosphere dew point were applied to the sintering of aluminium (Liu *et al.*, 2008; Schaffer and Hall, 2002)

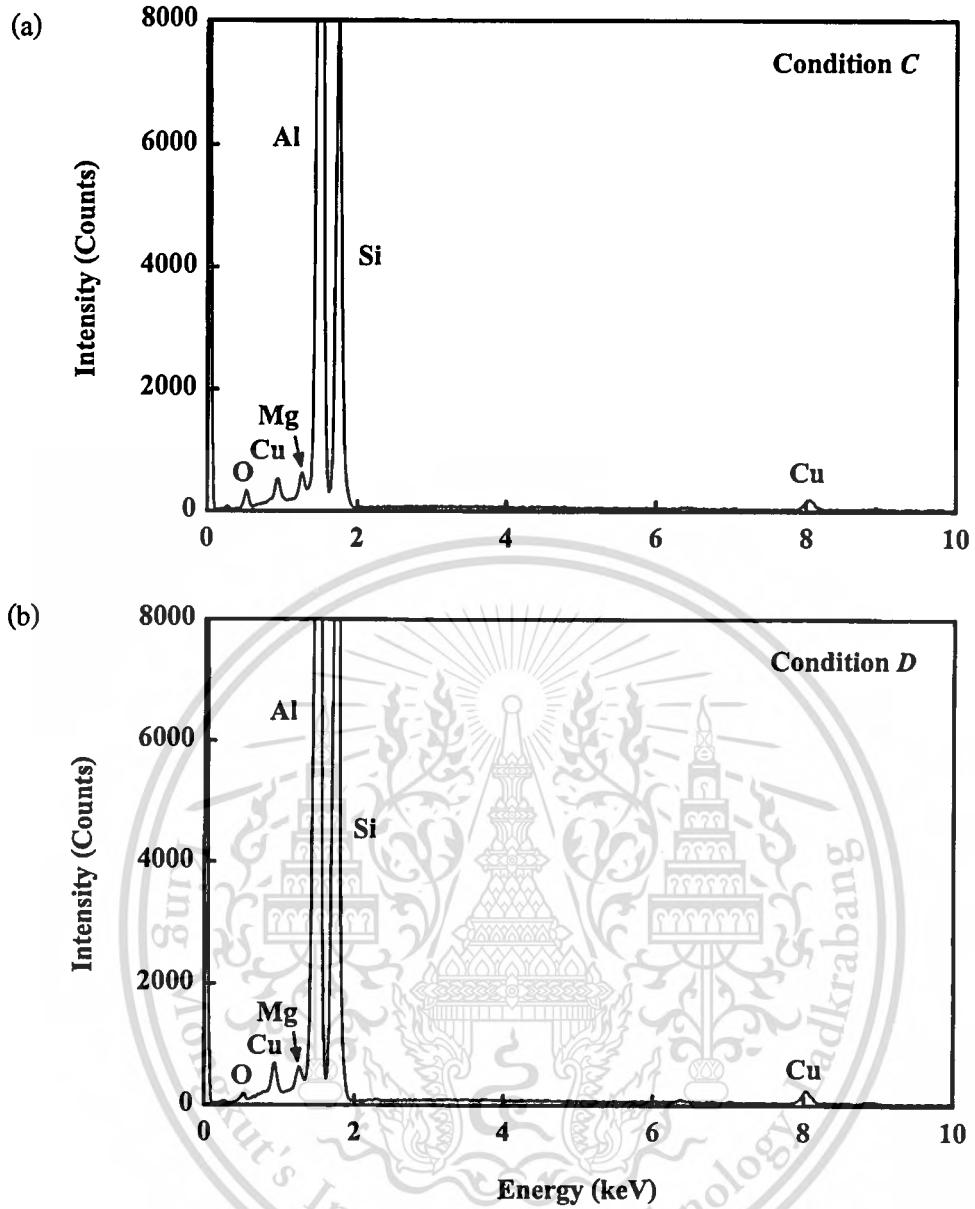

Figure 4.6 Energy dispersive spectrum (EDS) analysis at the centre of the sintered specimens obtained from (a) condition *C* and (b) condition *D*.

4.2.4 Oxygen contents

The relative O/Al contents measured at the centre of the specimens that were sintered in various conditions are shown Figure 4.7. By comparing with their green stage, it was found that the O/Al contents observed on the sintered specimens were increased for the specimens sintered in conditions *A*, *B* and *C*. The specimens sintered in condition *A* gained the most amount of oxygen during sintering, while these contents observed on the specimens sintered in conditions *B* and *C* were similar but lower than condition *A*. The specimens sintered in condition *D*

contained the lowest O/Al contents and their value was found to be even lower than that observed on the green specimens. The reduction of oxide for the sintering condition *D* was dominantly by magnesium (Neubing *et al.*, 2002). There was no evidence of reduction by nitrogen as already shown in Figure 4.6 (b). Another factor that caused the improved sinterability, was the self-getteing phenomenon. The atmosphere of sintering in condition *D* had the lowest dew point and low oxygen contents because the sintering chamber was flushed with 99.999% purity nitrogen gas for 12 hours before sintering. This minimised the residual moisture and oxygen and others impurities within the chamber. Therefore, self-gettering by the water vapour and oxygen was not severe.

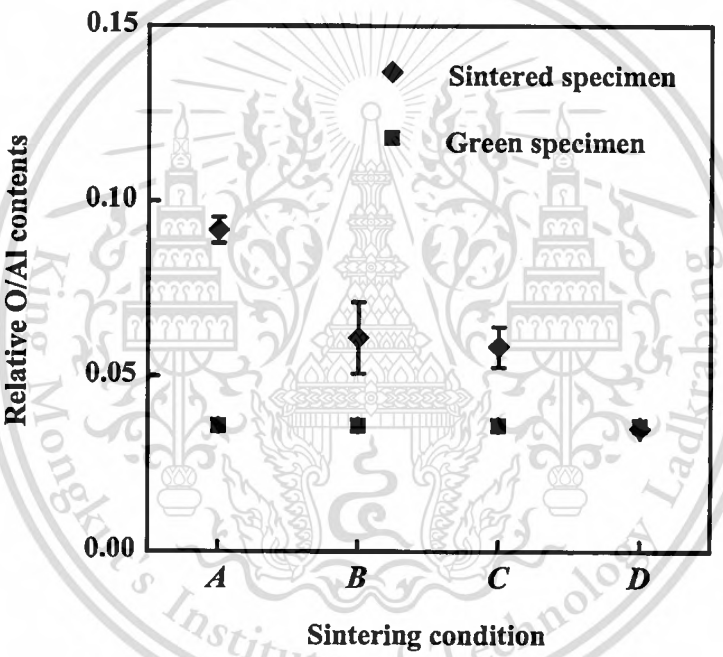

Figure 4.7 The relative oxygen per aluminium contents measured at the centre of both green and sintered specimens cross section.

4.3 Effects of Sintering Conditions on Mechanical Properties

4.3.1 Macroscopic Hardness

Figure 4.8 illustrates the effects of sintering conditions on the macroscopic hardness of the specimens. Initially, the hardness test was taken on the specimen surface. The highest hardness of 74 HRF was observed on the specimens sintered in condition *D*, while the specimens sintered in conditions *C*, *B* and *A* gave the similar hardness results, which were 58, 57, and 53 HRF respectively. The hardness of conditions A, B and C was not in agreement with the

microstructures result as shown in Figure 4.5 (b)-(d). However, it was found that the hardness measured on the specimens surface was not suitable because of the poor sinterability at the surface due to the self-gettering phenomenon. Therefore, the hardness values were lower than normal. The hardness was measured again at the centre of the specimens and the result was significant higher than that measured at the surface for the specimens sintered in conditions *B*, *C*, and *D*. For condition *A*, it was found that the hardness measured at both centre and surface was similar. This is in agreement with the microstructures observed on both positions. Similar results were also reported by Casella *et al.* (2004), who measured the microscopic hardness from the specimen surface to the centre and found that the significantly higher of the hardness was observed on the centre. In addition, the hardness measured at the centre agrees well with the density and shrinkage obtained previously.

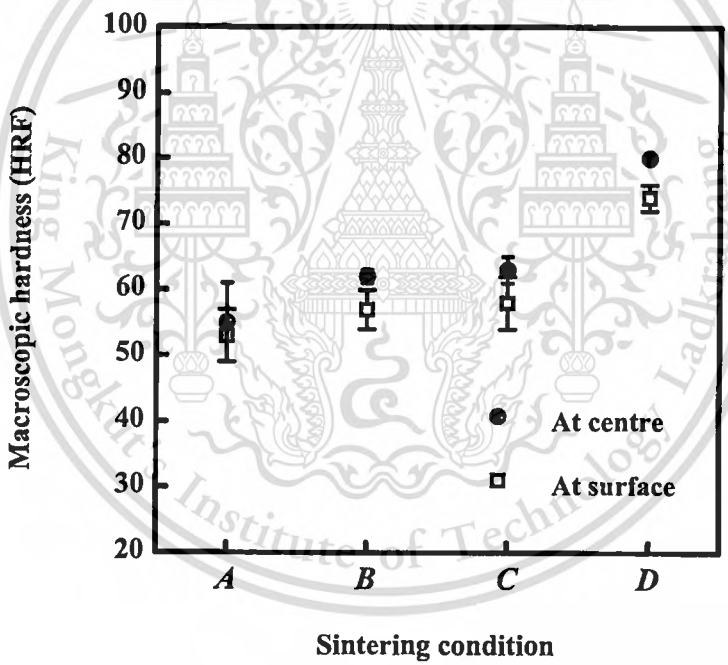

Figure 4.8 Rockwell hardness of the specimen as a result of sintering conditions.

4.3.2 Tensile Properties

In addition, the corresponding tensile properties of sintered specimens are illustrated in Figure 4.9. This indicates that both tensile strength and elongation were dependent on the atmosphere dew point. Sintering in the highest atmosphere dew point, the lowest tensile strength of 100 MPa and elongation of 0.5% was observed. This was due to partial sintering of the powder resulted from the prevention of pore minimisation by the moisture in the atmosphere.

As the atmosphere dew point decreased both tensile strength and elongation were improved because the powders were more densified. Until the atmosphere dew point reached the maximum value in this experiment, the highest tensile strength of 171 MPa with 1.6% of elongation were observed. Both tensile strength and elongation also showed the results in agreement with the physical properties as observed previously.

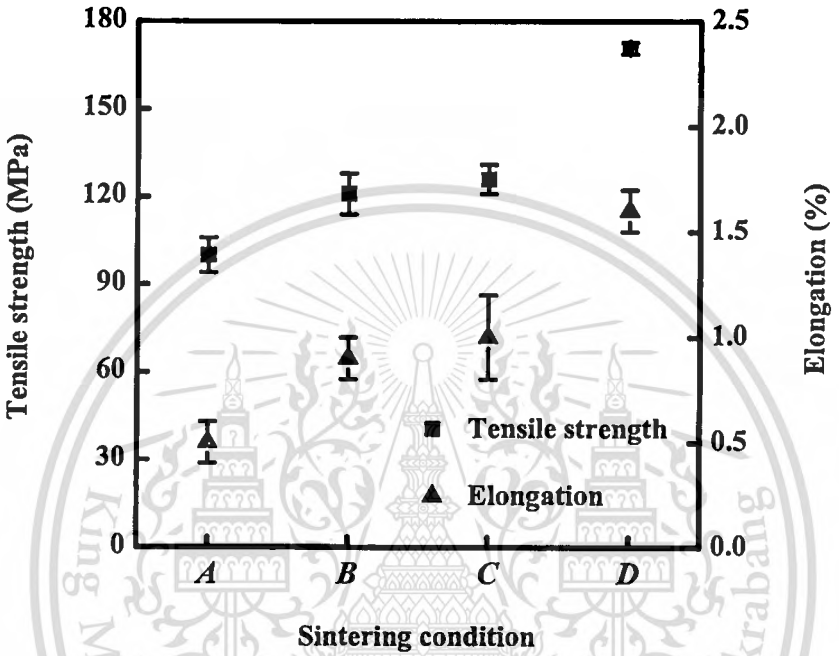

Figure 4.10 Tensile strength and elongation of the specimens as a result of sintering conditions.

4.4 Experimental Conclusion

In summary, the sintering conditions affected directly the atmosphere dew point and hence affected the sinterability of Al-Si-Cu-Mg powder. Sintering in the lower atmosphere dew point showed the better physical and mechanical properties. During sintering in various conditions, aluminium alloy powder exposed to various levels of moisture, resulting in different sinterability. Sintering of aluminium alloy was achieved by the presence of magnesium. The role of magnesium was to reduce the oxide of aluminium and then exposed the fresh aluminium to sinter with each other. If the level of moisture was high, it was possible that the exposed aluminium could be re-oxidised with the moisture and hence gain the oxide from the moisture. This resulted in poor sinterability as evidenced by the low physical and mechanical properties. While if the level of moisture was low, the re-oxidised of exposed aluminium was less severe due to the self-gettering phenomenon, in which the aluminium powders at the surface acted as the getter for the

inner section. Therefore, if the sintering atmosphere had too high level of moisture, the reduction by magnesium and self-gettering was not effective because the oxidation rate of aluminium with moisture was faster than that with oxygen. The reduction by self-gettering was not enough and the partial pressure of water vapour was still high within the inner section. This caused the specimens has poor sinterability. For the specimens sintered in the lower atmosphere dew point, the moisture in the atmosphere was low enough to be reduced or consumed by the aluminium powders at the surface. In this case, the water partial pressure in the inner section was low and allowed the powders to sinter better.

CHAPTER 5

THE EFFECTS OF COMPACTION PRESSURES ON SINTERABILITY OF Al-Si-Cu-Mg ALLOY

5.1 Effects of Compaction Pressures on Physical Properties

5.1.1 Density

The relative densities of the green specimens with various compaction pressures are shown in Figure 5.1. It shows that the green density was rapidly increased from the initial apparent density of 44-75% theoretical density (% TD) when the pressure of 150 MPa was applied. When the compaction pressure was increased, the green density was increased but in the slow rate. In this experiment, the maximum compaction pressure exerted on the aluminium alloy powder was 700 MPa with the obtained relative density of 93.6% TD.

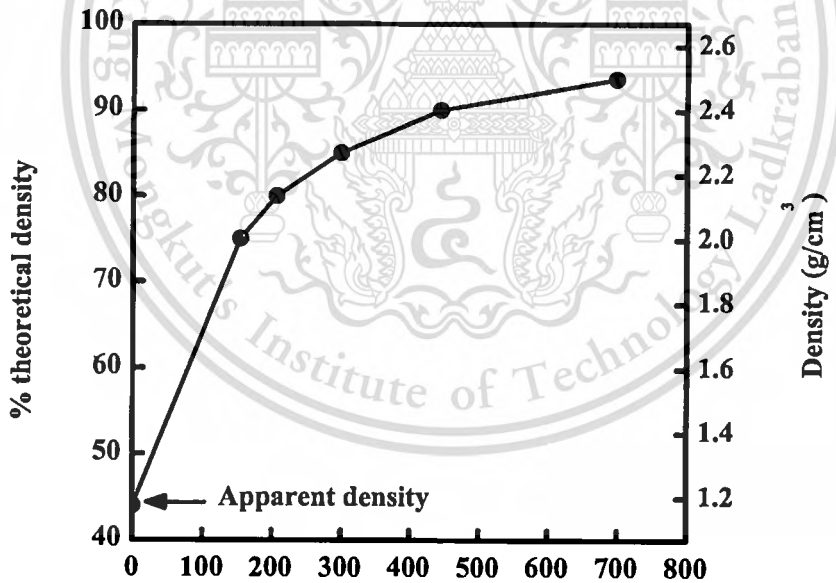

Figure 5.1 Green density resulting from various compaction pressures.

The rate of change of green density with respect to compaction pressure is shown in Figure 5.2. It was found that as the compaction pressure increased from 0-300 MPa, the rate of change of green density was change fast from 44-85% TD. While the compaction pressure increased from

300-700 MPa, the density was changed from 85-93.6% TD with the slow rate of change. At this region, even the high compaction pressure was applied, the slightly change of density was observed. Therefore, the compaction pressures used in this study can be separated into two ranges, namely the low pressure, regarding 150-300 MPa and the high pressure, regarding 300-700 MPa.

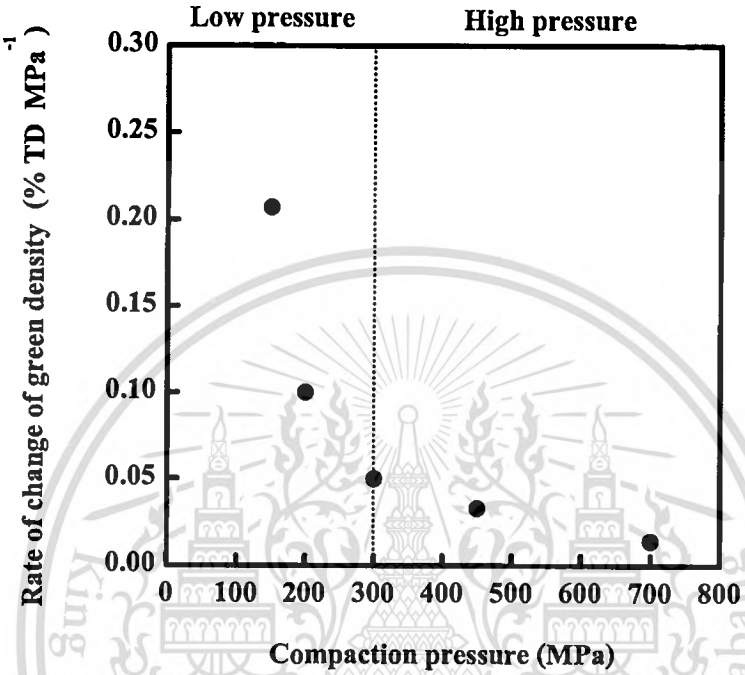

Figure 5.2 Rate of change of green density with respect to the compaction pressure.

From Figure 5.2, at the low compaction pressure range, the rapid increase in green density was mainly due to the rearrangement of powder and localised deformation (German, 1994). At the beginning, the powder had a density approximately equal to the apparent density. As pressure applied, the first response was the rearrangement of the particles to fill large spaces, giving a higher coordination. Increasing pressure produced better packing and led to decrease porosity by localised deformation at the powder contacts. At the high compaction pressure range, the increasing in density is mainly due to the contact enlargement to reduce porosity through plastic deformation only. Therefore, the rate of increase in green density was slow.

Figure 5.3 shows the green and sintered densities of the specimens compacted using various compaction pressures. The relative density was increased from 75% TD for green to 96.6% TD for sintered if the specimens were compacted with 150 MPa. The sintered density was increased as the compaction pressure increased. On the other hand, the specimens compacted at 700 MPa had the green density of 93.6% TD and the sintered density of 98.3% TD. As a result from the green

density, the specimens compacted with the high pressure, the high sintered density was obtained. It was mainly because the high compaction pressure increased the number of particle contacts through plastic deformation and consequently enhanced the sintering rate.

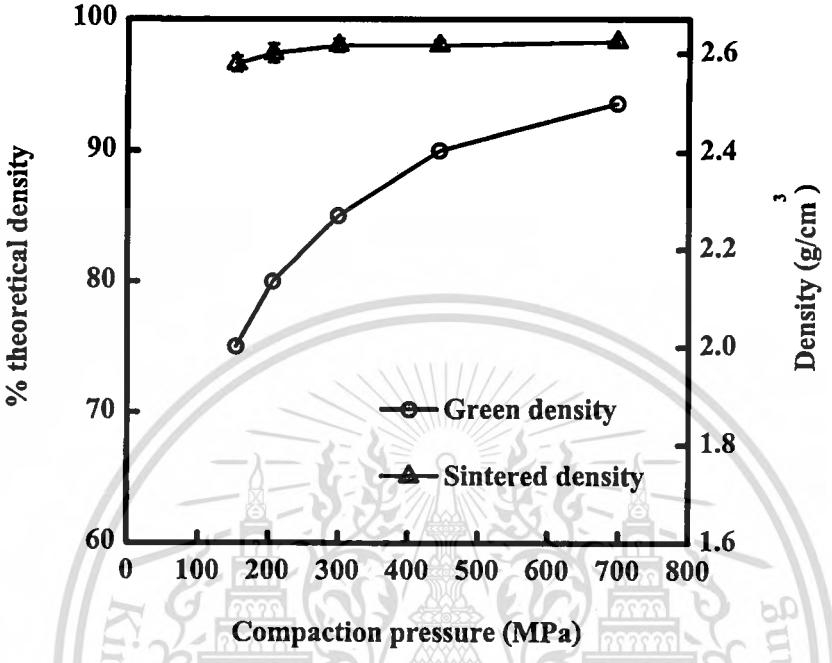

Figure 5.3 Sintered density with respect to various compaction pressures comparing with their green density.

From Figure 5.3, the increase in density from green to sintered stages can be calculated from the density difference between sintered density and green density ($\rho_s - \rho_g$) and the result is shown in Figure 5.4. It shows that the specimens compacted at the low compaction pressure range had large increase in density, while the specimens compacted with the high compaction pressure range had less increase in density.

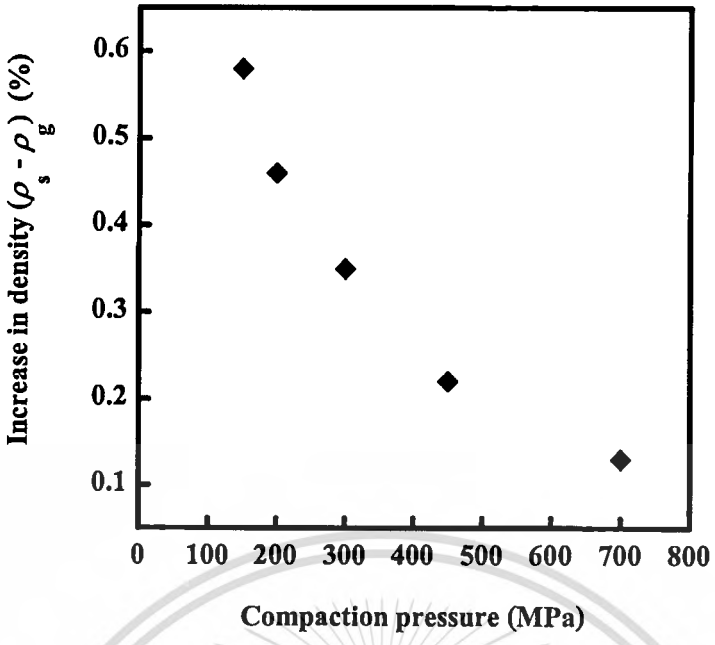

Figure 5.4 The increase in density after sintering for varied compaction pressure.

5.1.2 Dimensional Change

The density results showed that all sintered densities were higher than their corresponding green densities, which indicated that there was shrinkage occurred. The shrinkage of the specimens at particular position is shown in Figure 5.5. It shows that the specimens compacted with the low compaction pressure shrank more than those compacted with the higher compaction pressure at all measured positions. It also shows the uniform shrinkage at W_1, W_2, and W_3 as illustrated in Figure 5.5 (a). Their average shrinkage, $W_{average}$ is shown in Figure 5.5 (b). Moreover, it was found that the shrinkage of these three positions and their average value were also similar to the L position as shown in Figure 5.5 (c). Therefore, this can be said that that all positions in the direction perpendicular to the pressing direction showed the uniform shrinkage. However, in the direction parallel to the pressing direction, T, the shrinkage was relatively higher for the specimens compacted at the lower compaction pressure (150-300 MPa) and relatively lower for those compacted at the high compaction pressure (300-700 MPa) as shown in Figure 5.5 (d).

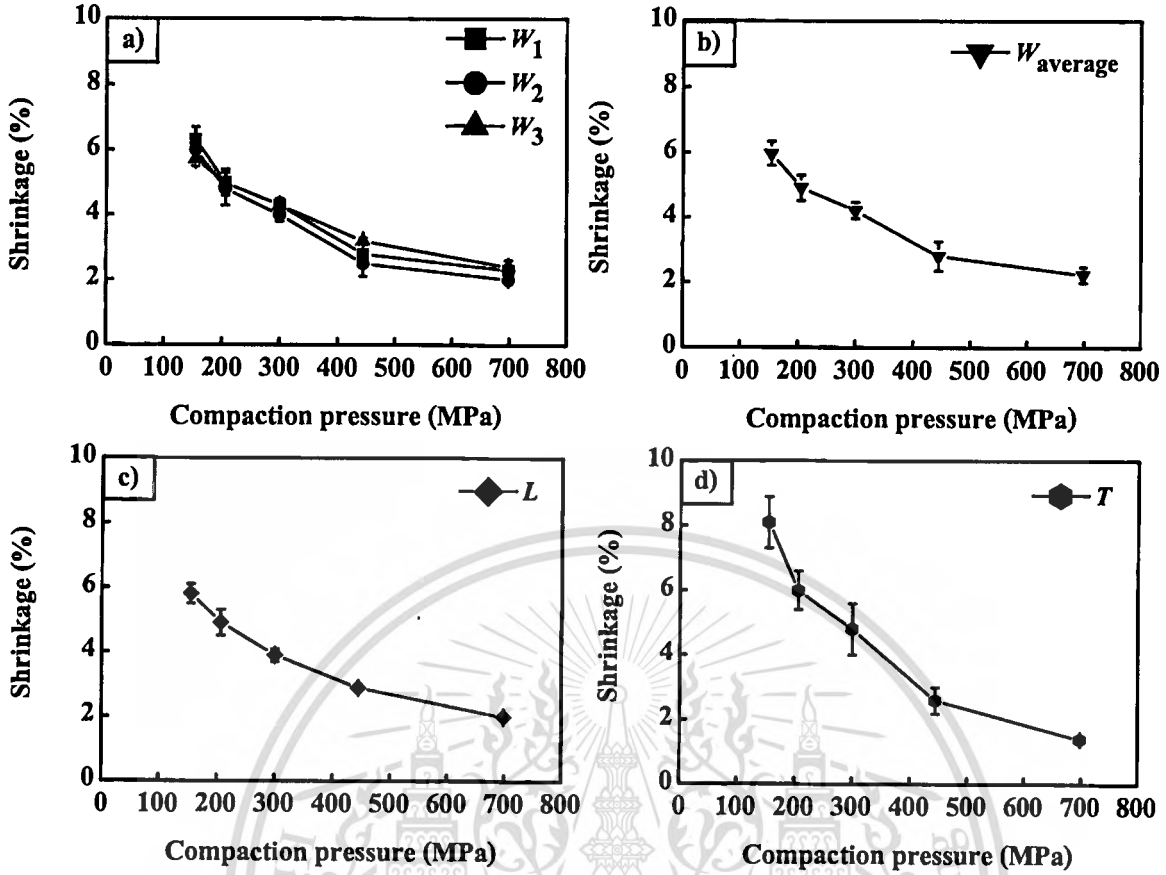

Figure 5.5 Effects of compaction pressures on the dimensional change at different positions of the sintered specimens with respect to their green dimension.

This can be explained that the aluminium powders undergo deformation during compaction. In the case of low compaction pressure, the aluminium powders were less deformed and less contact areas between powders led to more and larger pores distributed in the specimens as shown in Figure 5.6 (a). On the other hand, large deformation and consequently large contact areas were found on the compacts formed by high compaction pressure, hence, these compacts contained less and smaller pores as shown in Figure 5.6 (b). After sintering, it was found that, the specimens from all compaction conditions reached the sintered density higher than 96% TD and up to 98.3% TD. This was because of the high shrinkage occurred on the specimens compacted by the low pressure and less shrinkage by the high pressure. However, the shrinkage of the specimens still showed the non-uniformity between the directions perpendicular and parallel to the pressing direction. The specimens compacted by the low pressure showed the higher shrinkage in the direction parallel to the pressing direction than that in the direction perpendicular to the pressing direction. While the specimens compacted by the high pressure showed the result in the opposite way. This opposite relation can be

explained by using the density gradient, especially for the specimens compacted by low pressure had higher thickness than those compacted by high pressure. An increase in the height resulted in greater density gradient and lower green density. However, the amount of shrinkage varied inversely with the green density. Therefore, a low green density resulted in a larger shrinkage. While the specimens compacted in the high pressure range, the effects of density gradient were less and the results were similar to the previous experiment.

5.1.3 Microstructures

Figure 5.6 (a) shows the microstructures of the green specimens compacted at the lowest compaction pressure (150 MPa) and Figure 5.6 (b) for the highest compaction pressure (700 MPa) respectively. After sintering, the microstructures of the all compaction conditions are presented in Figure 5.7. The microstructures were similar for all compaction pressures in which the silicon phase dispersed homogeneously throughout the aluminium matrix as shown in Figure 5.7 (a)-(e) and the pores were rarely be seen. Figure 5.7 (f)-(j) shows the microstructures observed at the superficial region. The sinterability was poorer at the superficial region comparing to that at the central region. There were more pores distributed near the surface, which directly affected the hardness of the specimens. However, as the compaction pressure increased the pore size and number of pores in the superficial region was also decreased in a similar manner as the central region.

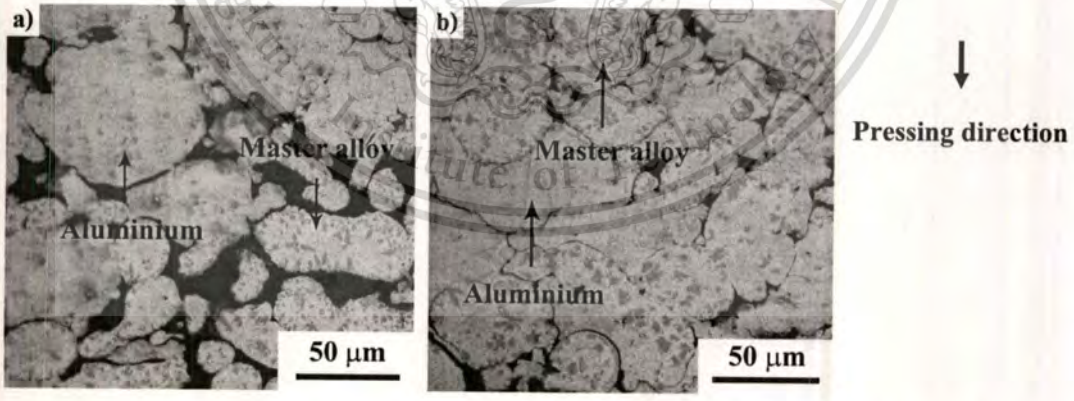

Figure 5.6 Microstructures of the green specimen compacted by (a) 150 MPa and (b) 700 MPa.

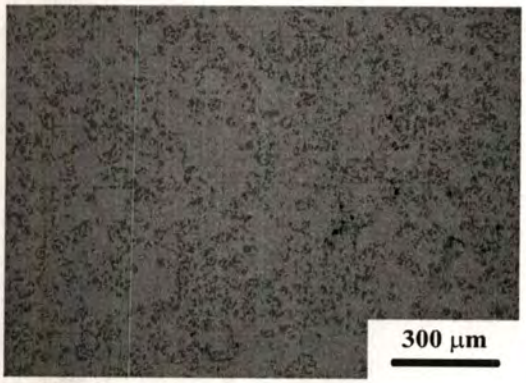

(a) 150 MPa (Centre)

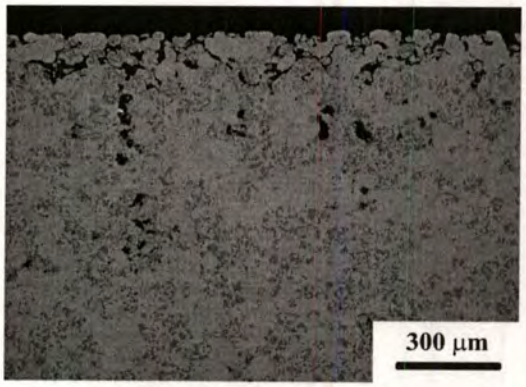

(f) 150 MPa (Superficial)

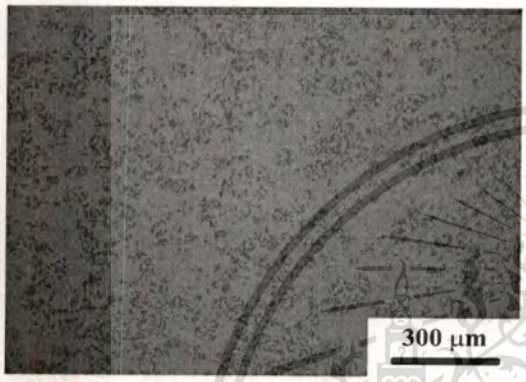

(b) 200 MPa (Centre)

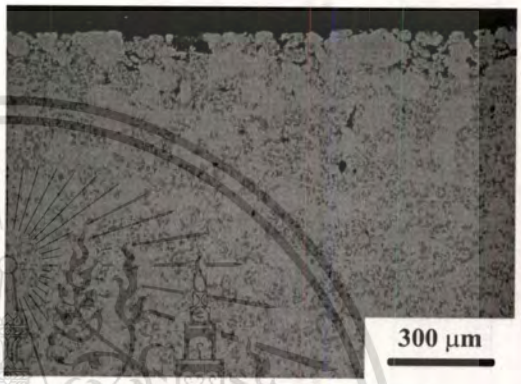

(g) 200 MPa (Superficial)

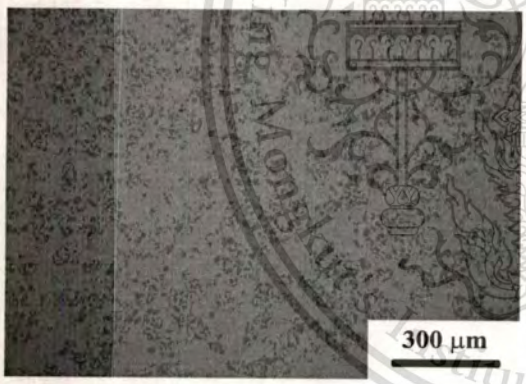

(c) 300 MPa (Centre)

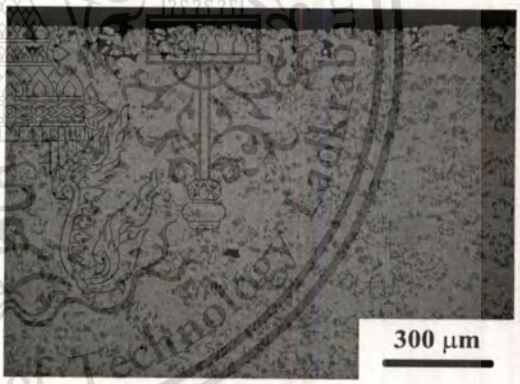

(h) 300 MPa (Superficial)

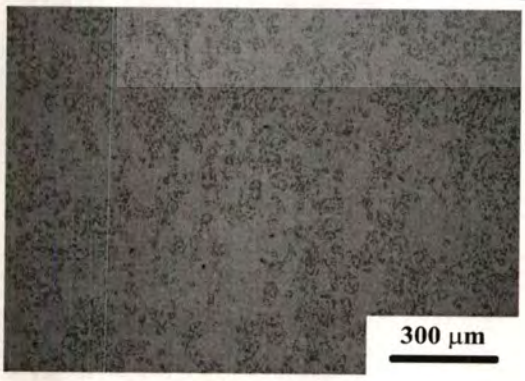

(d) 450 MPa (Centre)

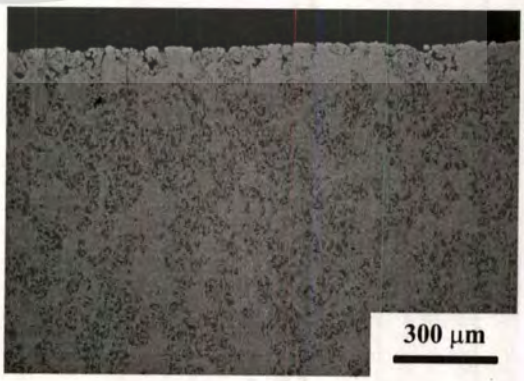

(i) 450 MPa (Superficial)

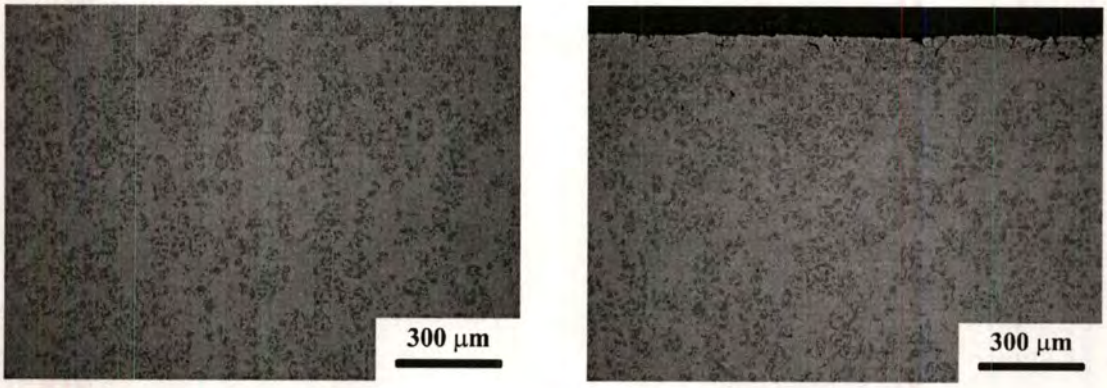

(e) 700 MPa (Centre) **(j) 700 MPa (Superficial)**

Figure 5.7 Microstructural images of the sintered specimens compacted at different compaction pressures, (a) and (f) 150 MPa, (b) and (g) 200 MPa, (c) and (h) 300 MPa, (d) and (i) 450 MPa, and (e) and (j) 700 MPa. (a)-(e) shows the central region, while (f)-(j) showed the superficial region.

From the microstructural results, it was in agreement with the density and dimensional change results, in which the specimen showed the well sintered microstructures at the centre in all compaction conditions. However, there were still the pores, which indicated the poor sinterability at the superficial region due to the self-gettering effect (Schaffer and Hall, 2002). The superficial region with pores became thinner as the pressure increased because the compacted specimens were densed and it was more difficult for the oxygen and moisture to pass through the inner section of the specimen.

The EDS analysis at the central region of the sintered specimens compacted at 150, 300, and 700 MPa, is shown in Figure 5.8 and there is no evidence of the oxide reduction by nitrogen as discussed in section 4.2.3 (Schaffer and Hall, 2002; Schaffer *et al.*, 2006).

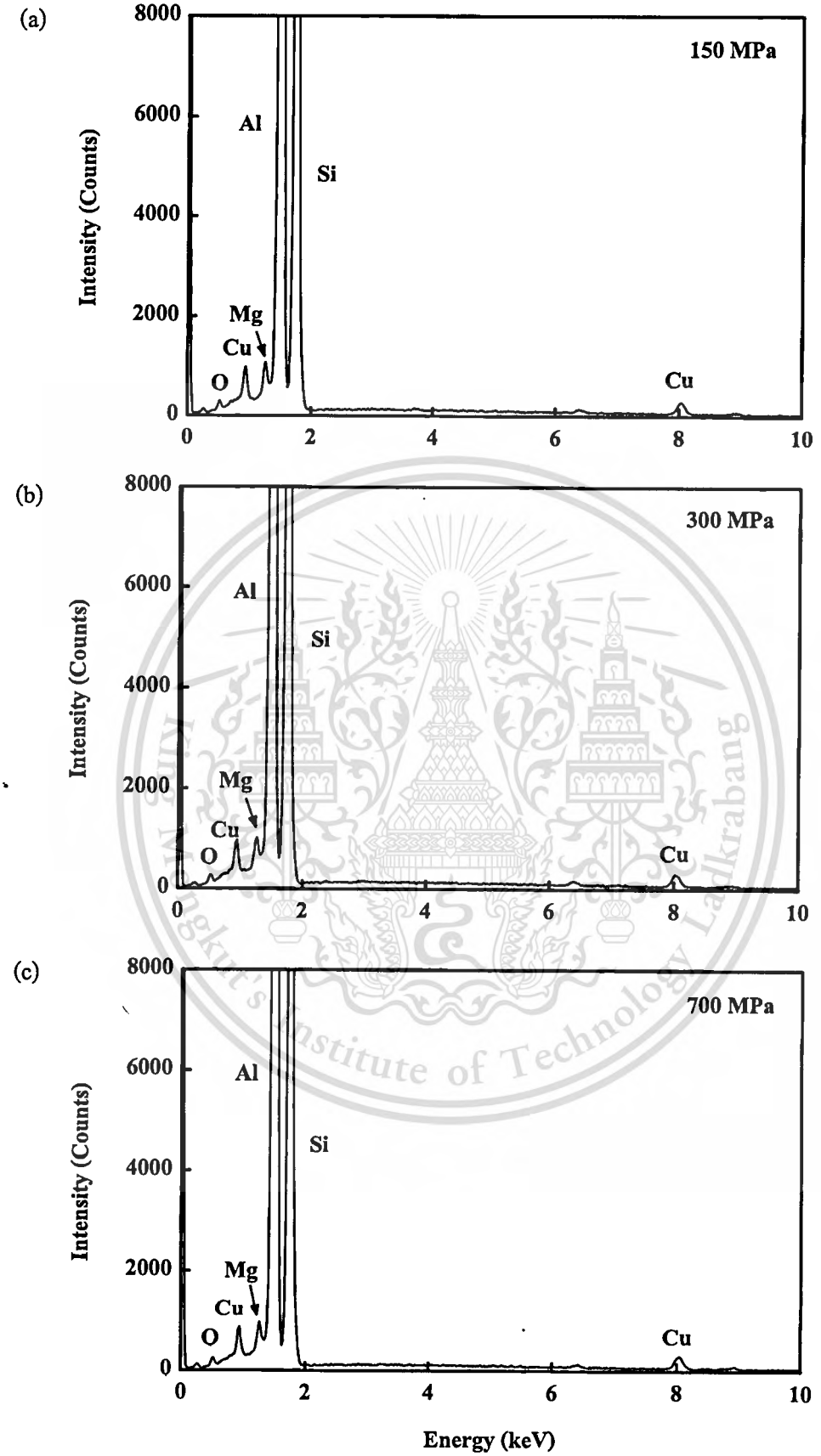

Figure 5.8 EDS analysis at the centre of the sintered specimens compacted at (a) 150 MPa, (b) 300 MPa, and (c) 700 MPa.

5.1.4 Oxygen Contents

Figure 5.9 shows the relative O/Al contents of the green and sintered specimens measured at centre. It shows that these contents in the sintered specimen were slightly reduced from its green state at all conditions. The specimen compacted at the lowest compaction pressure (150 MPa) contained the highest O/Al contents. When the compaction pressure was increased to 200 MPa, these contents were lower but remained relative constant there after. The tendency of the result was similarly in both green and sintered state.

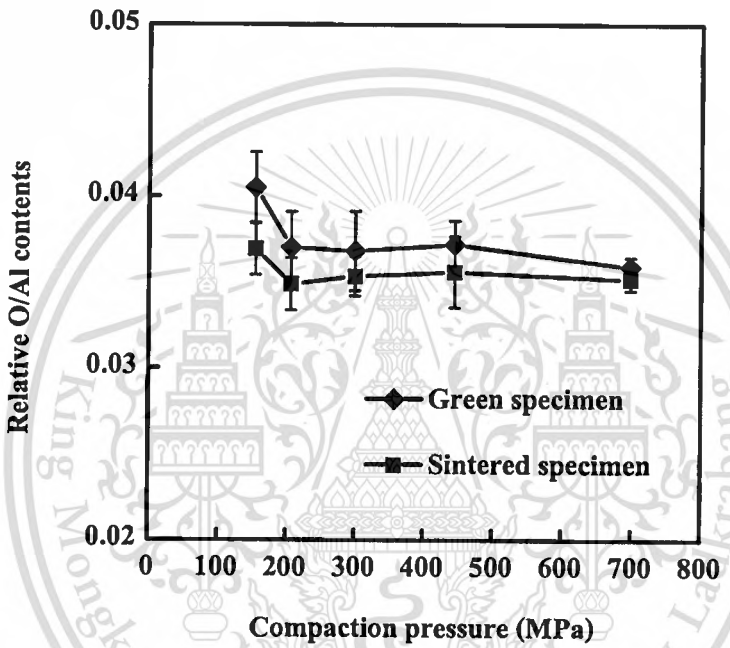

Figure 5.9 The relative O/Al contents measured at the centre of both green and sintered specimens cross section as a function of compaction pressure.

From the literatures in section 2.2.2.2, the role of compaction pressure is to rupture the oxide layers of aluminium powder, thus, the O/Al contents measured on the green specimens should be constant. However, the results of the O/Al contents show the lower contents on the green specimens when the compaction pressure increased from 200 MPa. It can be explained by using the film rupture mechanism during compaction (Andreeva and Rastrigina, 1966) that the rupture of the oxide layers was accomplished by the plastic deformation of aluminium powders, their contact areas were increased. The oxide layers could not retain when the particle surface changed and the oxide layers broke up into fragments, forming cracks in between when pure metal appeared. During subsequent deformation, the cracks began to spread and contact bridges were formed in the zones of film rupture.

Consequently metallic contact was achieved through a network of bridges. This indicated that the specimens compacted by low compaction pressure had less deformation as observed on the microstructure in Figure 5.6 (a), hence the less oxide rupture. In addition, it was possible to have the non-deformed powders within the specimen, therefore, the high O/Al contents value was observed. While increasing the compaction pressure, the aluminium powders underwent large deformation and their surface areas increased. The cracks were formed and subsequently the oxide layers were spread out by the spreading metal and contact bridges to form in the zones of oxide rupture. Therefore, the slightly lower of O/Al contents was due to the increase in oxide free zones, where the oxide layers were spread out.

After sintering, it is found that these contents were slightly lower than those observed on their green specimens. This indicated that there was the oxide reducing mechanism occurred during sintering. The reduction of oxide did not depend on the increase in the compaction pressure as the difference in O/Al contents was similar for all compaction pressures. The compaction pressure could only rupture the oxide layers. Therefore, the oxide reduction was caused by magnesium similar to the previous experiment (Neubing *et al.*, 2002). The slightly reduction of O/Al contents suggested that the oxide was reduced only by magnesium but not by nitrogen as evidenced by EDS analysis.

According to the self-gettering phenomenon, the aluminium powders at the surface acted as the getter for those in the inner section. Therefore, the aluminium powder in the outer layer got more oxygen than those inside the specimen. This caused the lowers oxygen partial pressure in the inner section and allowed the aluminium powders to sinter better. Figure 5.10 shows the proof of the self-gettering phenomenon on the specimen compacted at 150 MPa by measuring the O/Al contents from the centre to the surface. The results show that these contents at the region near the centre were constant, while the near surface region, these contents was rapidly increasing. Pieczonka *et al.* (2007) also found that the percentage by weight of oxygen was 4 times higher at the surface than that at the centre of pure aluminium sintered specimens caused by self-gettering phenomenon.

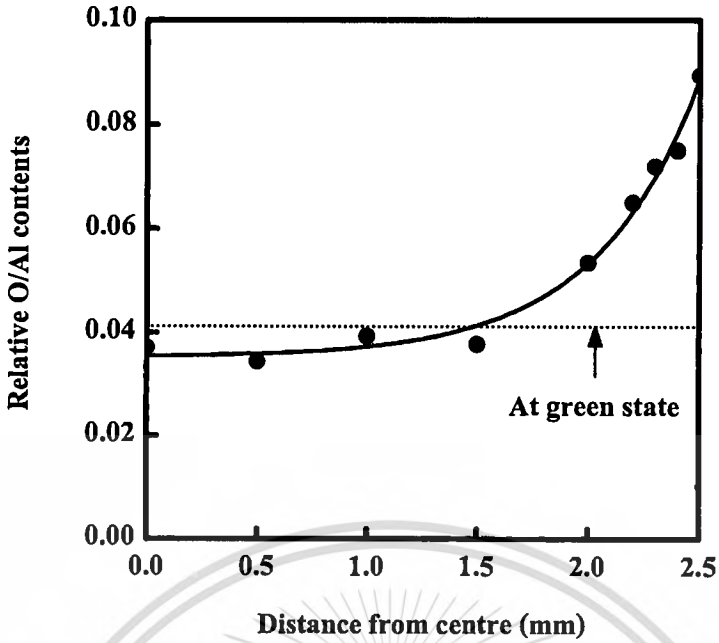

Figure 5.10 The relative O/Al contents of the sintered specimens compacted at 150 MPa measuring from centre to the surface. Dash line indicates the oxygen contents at green state.

5.2 Effects of Compaction Pressures on Mechanical Properties

5.2.1 Macroscopic Hardness

Figure 5.11 shows the macroscopic hardness results of the specimens as a function of compaction pressure. Initially, the test was taken on the specimen surface and it showed that at the low compaction pressure range, the hardness was increased from 59 to 71 HRF. When the compaction pressure increased to the high pressure range, the trend of hardness was constant at the average value of 72 HRF. The results are similar to the trend of density results.

As similar to the previous experiment, the microstructures of the specimens still showed the poor sinterability at superficial region affected by the self-gettering phenomenon. Therefore, the hardness was also measured at the centre of all specimens and their results are also shown in Figure 5.11. The hardness at the centre showed the higher value relative to that at surface which indicated that sintering was better at centre. This is supported by the microstructural images in Figure 5.7 (a)-(e).

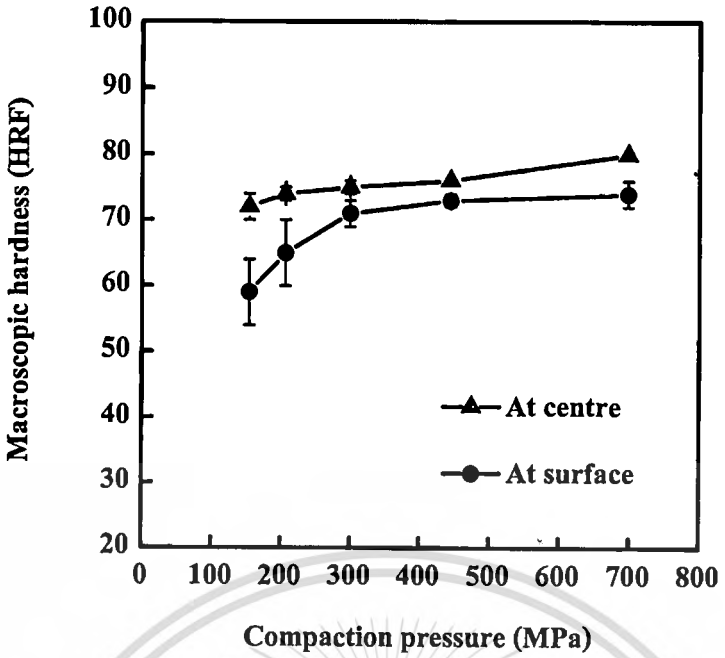

Figure 5.11 Rockwell F-scale hardness of specimens as a function of compaction pressure.

5.2.2 Tensile Properties

Tensile properties including tensile strength and elongation of the specimens are illustrated in Figure 5.12. The tensile properties had similar trend as the hardness at both centre and surface. As the compaction pressure increased, both tensile strength and elongation were increased. The maximum values were obtained from the specimens compacted at 700 MPa, which was 171 MPa for the tensile strength and 1.6% for elongation, while the minimum were 125 MPa for tensile strength and 1.0% for elongation obtained from the specimens compacted at 150 MPa.

According to the tensile properties, it shows that as the compaction pressure increased, the tensile strength and elongation were increased, which was similar to the density and hardness results. However, the hardness results at the surface showed the relatively large deviation, but the elongation results showed the less deviation for the specimens compacted by low compaction pressure. The large deviation of the hardness was from the poor sinterability of the specimens surface due to the self-gettering phenomenon, but the microstructure at centre showed the well sintering and the corresponding hardness measured at this region showed less deviation. Therefore, the elongation and the hardness at centre of the specimens had similar deviation.

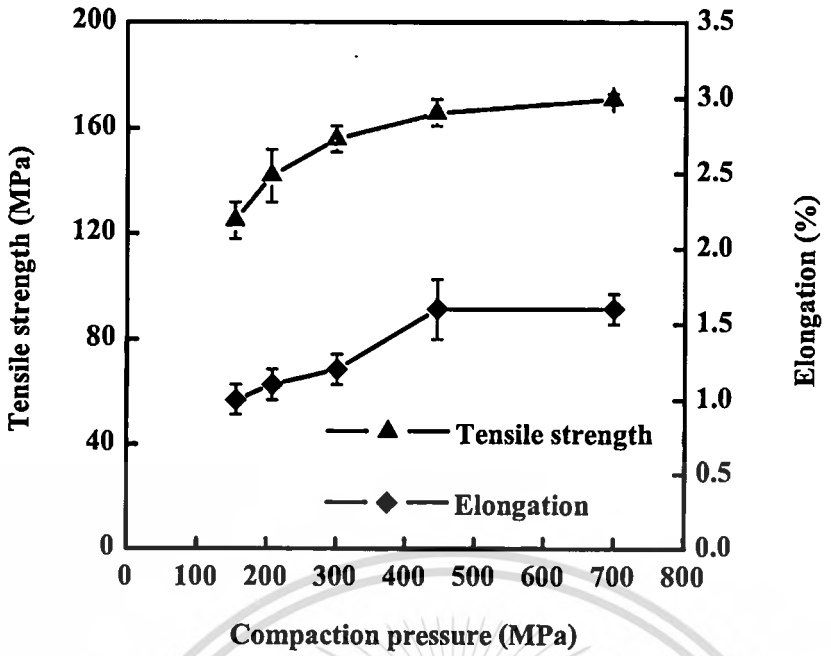

Figure 5.12 Tensile strength and elongation as a function of compaction pressure.

5.3 Experimental Conclusion

In conclusion, the compaction pressure affected directly to the sinterability of Al-Si-Cu-Mg alloy by enhancing both physical and mechanical properties. At the low compaction pressure region, the green density rapidly increased due to the powder rearrangement to fill the large pores and packed together with the adjacent particles. As the compaction pressure increased, the green density was increased because the powders were more deformed to increase the surface areas, leading to pore minimising. However, at the high compaction pressure range, the density change was slightly due to the powders were plastically deformed and work hardened. The sintered density of all compacted conditions was increased from their green density and showed the value ranging from 96.6-98.3% TD. The shrinkage results showed that as the compaction pressure increased, the shrinkage was decreased but the shrinkage was still non-uniform. The microstructures showed the corresponding features to the shrinkage, in which the sintering was better at centre for all conditions. This corresponded to the fact that the shrinkage was high for the specimens compacted by the low pressure. However, the poor sinterability at superficial region was still observed for all specimens due to the self-gettering phenomenon. The effects of self-gettering was lower as the higher compaction pressure was applied because the compacts had more densed, therefore, the oxygen or moisture in the atmosphere could not penetrate in to the deep inside the pore easily. The oxygen contents analysis showed the slightly reduction of oxygen contents in the sintered specimens, which suggested that the reduction mechanism

of oxide was dominantly by magnesium and there was no evidence of oxide reduction by nitrogen. In addition, the mechanical properties showed the similar results to the trend of sintered density. From all results, it can be suggested that it is possible to form the aluminium powder components from the initial low green density but the main problem is the self-gettering phenomenon that causes the compacts to have poor properties. Therefore, this problem can be solved by sintering in the lower atmosphere dew point.

CHAPTER 6

CONCLUSION AND SUGGESTIONS

6.1 Conclusion

Sintering conditions can affect atmosphere dew point and hence can significantly influence the sinterability of Al-Si-Cu-Mg alloy. The best sintering condition observed in this experiment was the flow controlled 99.999% purity of nitrogen gas by using the tube furnace with the appropriated flow rate of gas. The dewaxing and sintering temperatures were 420 and 560°C respectively and the sintering time was 60 minutes. Using the best condition for sintering, the sintered density was 98.3% theoretical density. The linear shrinkage was highest amounts other sintering conditions. However, the shrinkage was not uniform because of the nature of specimens that were compacted uniaxially. The tensile strength of 171 MPa with the 1.6% of elongation could be obtained. The macroscopic hardnesses measured at the surface and centre of specimens were 74 and 80 HRF respectively. Microstructures showed the duplex microstructure that consisted of the silicon phase dispersed in the aluminium matrix. However, the specimens were well sintered at the centre but poor at the superficial region due to the self-gettering phenomenon. The main factor that influenced the properties was an atmosphere dew point, in which -38.4°C of atmosphere dew point could be reached by using the best sintering condition. Sintering in the atmosphere with low dew point enhanced densification of the Al-Si-Cu-Mg powder. If the atmosphere dew point was low enough, the oxide layers were reduced during sintering and this allowed the exposed aluminium to be sintered together. In contrast, continuing oxidation was re-occurred to the exposed aluminium, resulting in gaining more oxygen in high moisture environment. Therefore, sintering was hindered and poor sinterability was obtained.

The compaction pressure is another factor that can enhance sinterability of Al-Si-Cu-Mg alloy. The effect of compaction pressure could be separated into two ranges, the low and high pressure ranges. At the low compaction pressure, namely 0-300 MPa, the green density was rapidly increased from 44 to 85% TD. While applying the higher compaction pressure from 300-700 MPa, the green density was gradually increased from 85 to 93.6% TD. After sintering with the best condition obtained from the previous experiment, the sintered density was reached 96.6-98.3% TD. The increase in density from green to sintered stage was evidenced by the linear shrinkage and microstructures. The linear shrinkage was higher for the specimens compacted with the low pressure and vice versa. The

microstructures at the centre of all specimens showed the similar structures, in which a number of pores were less when compared with the superficial region resulting from the self-gettering phenomenon. However, the effects of this phenomenon were less pronounced as the compaction pressure increased, in which the layer of large pores distributed at the superficial region was reduced as the compaction pressure increased. At low green density, the oxygen or moisture in the atmosphere easily penetrated into the pore network and was consumed by the aluminium locating near the surface. Therefore, this layer of pores distributed at the superficial region affected the mechanical properties. The mechanical properties increased as the compaction pressure increased. In addition, the oxide analysis results indicated that the oxide was dominantly reduced by magnesium at all sintered specimens, when compared with the corresponding green specimens. However, there was no evidence of oxide reduction by the nitrogen because the partial pressure of oxygen was not low enough to activate that reduction.

6.2 Suggestions

Although this work was finished, it was only the first step towards aluminium injection moulding process. There are some suggestions to the work for further study towards injection moulding for aluminium as follow:

6.2.1 In order to reach the low dew point atmosphere, the gas flow rate should be comparable to the capacity of the sintering chamber. In addition, the self-gettering phenomenon is found to be a source of decreasing the mechanical properties. Therefore, an external gettering is required, in order to minimise the effects of self-gettering. The external getters may comprise any metal that has a higher affinity for oxygen and moisture than aluminium and does not vaporised at the sintering temperature of aluminium. Magnesium is geneally suggested (Liu, *et al.*, 2008) and hence, a few small pieces of it may be placed in the furnace surrounding the parts.

6.2.2 Another suggestion is on the appropriate binder for aluminium alloy to form a feedstock. From the literatures about aluminium injection moulding, the components of binder are kept in secret (Nishiyabu, *et al.*, 2004; Tan and Ma, 2004). However, there is only one work that gave the components of the binder used, but the moulded parts are solvent debinded prior to thermal debinding and sintering (Liu *et al.*, 2008). Solvent debinding is not recommended due to the environmental hazard. However, MIM process is currently a commercial process for titanium and titanium itself is also a reactive metal. Therefore, it is possible to use the binder that commonly used in titanium MIM.

6.2.3 Together with the above suggestion, the moulded parts have to be debinded prior to sinter. Debinding in air is seemed to be detrimental for aluminium. Therefore, the debinding process for aluminium should be carried out in the protective atmosphere or continuously with the sintering process to avoid the air exposure.

REFERENCES

1. Andreeva, N.G., Rastrigina, E.F. 1966. "Theory and Technology of Sintering, Heat Treatment, and Chemiothermal Treatment Process Mechanism of Metallic Contact Formation in SAP Type Alloys." Translated from **Poroshkovaya Metallurgiya**. 3 (39) : 27-36.

2. Apelian, D., Saha, D., 2000. "Aluminium P/M Processed Components-Challenges and Opportunities" 1-10. in Chernenkoff, R.A., Jandeska, W.F.Jr. **Powder Metallurgy Aluminium & Light Alloys for Automotive Applications Conference Proceedings**. New Jersey : Metal Powder Industries Federation.

3. ASM International. 1984. **ASM Handbook of Powder Metallurgy**. 7 : 381-385.

4. ASTM International. 2005. **Annual Book of ASTM Standards: Metallic and Inorganic Coatings; Metal Powders, Sintered P/M Structural Parts**. Vol. 02.05. Pennsylvania : ASTM International.

5. Carpenter, J.A. 2000. "Aluminium and Light Alloys for Automotive Applications Conference" 11-32. in Chernenkoff, R.A., Jandeska, W.F.Jr. **Powder Metallurgy Aluminium & Light Alloys for Automotive Applications Conference Proceedings**. New Jersey : Metal Powder Industries Federation.

6. Casella, D., Beltran, A., Prado, J.M., Larson, A., Romero, A. 2004. "Microstructural Effects on the Dry Wear Resistance of Powder Metallurgy Al-Si Alloys." **Wear**. 257 : 730-739.

7. Ciomek, M.A. **Feedstock and Processing for Metal Injection Moulding**. U.S. Patent No. 5064463. November 12, 1991.

8. Delarbre, P., Kerhl, M. 2000. "Aluminium and Light Alloys for Automotive Applications Conference." 33-39. in Chernenkoff, R.A., Jandeska, W.F.Jr. **Powder Metallurgy Aluminium & Light Alloys for Automotive Applications Conference Proceedings**. New Jersey : Metal Powder Industries Federation.

9. Djokic, S., Dubois, M., Lepard, R.H. **Process for the Production of Silver Coated Particles**. U.S. Patent No. 5945158. August 31, 1999.

REFERENCES (CONT.)

10. Dudas, J.H., Dean, W.A. 1969. "The Production of Precision Aluminium P/M Parts." **International Journal of Powder Metallurgy**. 5 (2) : 21-36.

11. ECKA Granulate GmbH. 2007. **ECKA Alumix 231, Press-Ready Mix for Aluminium Sintered Parts**. [Products Information]. Germany : ECKA Granulate GmbH & Co. KG.

12. Flumerfelt, J.F. 1999. "Aluminium Powder Metallurgy Processing." Ph.D. Thesis of Iowa State University.

13. Fuentes, J.J., Rodriguez, J.A., Herrera, E.J. 2003. "Effect of Mg as Sintering Additive on the Consolidation of Mechanically Alloyed Al Powder." **Materials Science Forum**. 426-432 : 4331-4336.

14. German, R.M. 1994. **Powder Metallurgy Science**. 2nd ed. New Jersey : Metal Powder Industries Federation.

15. German, R.M. 1996. **Sintering Theory and Practice**. New York : John Wiley and Sons.

16. German, R.M., Bose, A. 1997. **Injection Molding of Metals and Ceramics**. New Jersey : Metal Powder Industries Federation.

17. Gorner, W., Forster, H. 1995. "Determination of Oxide Film Thickness on Metal and Ceramic Materials Using Activation Analysis and B.E.T Gas Adsorption Method." **Journal of Radioanalytical and Nuclear Chemistry**. 192 (1) : 139-145.

18. Gray, J.E., Luan, B. 2002. "Protective Coatings on Magnesium and Its Alloys – A Critical Review." **Journal of Alloys and Compounds**. 336 : 88-113.

19. Griffith, W.M, Kim, Y.-W., Froes, F.H. 1986. "Powder Metallurgy Processing of Aluminium Alloy 7091." 283-303. in Fine, M.E., Starke, E.A.Jr. **Rapidly Solidified Powder Aluminium Alloys, ASTM STP 890**. Philadelphia, American Society for Testing and Materials.

REFERENCES (CONT.)

20. Gutin, S.S., Panov, A.A., Khlopin, M.I. 1972. "Effect of Oxide Films in the Sintering of Aluminium Powders." Translated from **Poroshkovaya Metallurgiya**. 112 (4) : 32-35.

21. Hu, C.-T. **Electroless Plating Method of Ni-Al Intermetallic Compound**. U.S. Patent No. 5458847. October 17, 1995.

22. Jangg, G., Danninger, H., Schroder, K., Abhari, K., Neubing, H.-C., Seyrkammer, J. 1996. "PM Aluminium Camshaft Belt Pulleys for Automotive Engines." **Materialwissenschaft und Werkstofftechnik**. 27 : 179-189.

23. Kim, D.H., Yoon, E.P., Kim, J.M. 1996. "Oxidation of an Aluminium 0.4 wt. % Magnesium Alloy." **Journal of Materials Science Letters**. 15: 1429-1431.

24. Kim, T.-S., Suryanarayana, C., Chun, B.-S. 2000. "Effect of Alloying Elements and Degassing Pressure on the Structure and Mechanical Properties of Rapidly Solidified Al-20Si-5Fe-2X (X=Cr, Zr, or Ni) Alloys." **Materials Science and Engineering**. 278A: 113-120.

25. Kimura, A., Kondoh, K., Shibata, M., Watanabe, R. 2001. "Breakaway Behavior of Surface Oxide Film on Aluminium-Silicon-Magnesium Alloy Powder Particles at High Temperature in Vacuum." **Materials Transactions**. 42 (7) : 1373-1379.

26. Krajnikov, A.V., Gastel, M., Ortner, H.M., Likutin, V.V. 2002. "Surface Chemistry of Water Atomised Aluminium Alloy Powders." **Applied Surface Science**. 195 : 26-43.

27. LaDelpha, A.D.P., Mosher, M.P., Caley, W.F., Kipouros, G.J., Bishop, D.P. 2008. "On the Simulation of Wrought AA4032 via P/M Processing." **Materials Science and Engineering**. 479A : 1-9.

28. Liu, Z.Y., Sercombe, T.B., Schaffer, G.B. 2008. "Metal Injection Moulding of Aluminium Alloy 6061 with Tin." **Powder Metallurgy**. 51 (1) : 78-83.

REFERENCES (CONT.)

29. Lumley, R.N., Sercombe, T.B., Schaffer, G.B. 1999. "Surface Oxide and the Role of Magnesium During Sintering of Aluminium." **Metallurgical and Materials Transactions.** 30A : 457-463.

30. Lutgens, F.K., Tarbuck, E.J. 1998. **The Atmosphere: An Introduction to Meteology.** 7th ed. New Jersey, Prentice-Hall International : 77-84.

31. Metal Powder Industries Federation. 2002. **Standard Test Methods for Metal Powders and Powder Metallurgy Products.** New Jersey : Metal Powder Industries Federation.

32. McLeod, A.D., Gabryel, C.M. 1992. "Kinetics of the Growth of Spinel, $MgAl_2O_4$, on Alumina Particulate in Aluminium Alloys Containing Magnesium." **Metallurgical Transactions.** 23A : 1279-1283.

33. Neikov, O.D., Krajnikov, A.V. 1996. "Water Atomized Powders of Aluminium and Its Alloys." **Material Science Forum.** 217-222 : 1649-1654.

34. Neubing, H.C., Gradl, J., Danninger, H. 2002. "Sintering and Microstructure of Al-Si P/M Components." **Advances in Powder Metallurgy and Particulate Materials.** 13 : 128-138.

35. Nishiyabu, K., Matsuzaki, S., Ishida, M., Tanaka, S., Nagai, H. 2004. "Development of Porous Aluminium by Metal Injection Moulding." **Materials Forum.** 28 : 376-382.

36. Ozbilen, S., Unal, A., Sheppard, T. 2000. "Influence of Atomizing Gases on the Oxide-Film Morphology and Thickness of Aluminium Powders." **Oxidation of Metals.** 53 : 1-23.

37. Pickens, J.R. 1981. "Review Aluminium Powder Metallurgy Technology for High-Strength Applications." **Journal of Materials Science.** 16 : 1437-1457.

REFERENCES (CONT.)

38. Pieczonka, T., Schubert, Th., Baunack, S., Kieback, B. 2007. "Dimensional Behavior of Aluminium Sintered in Different Atmospheres." **Materials Science and Engineering**. A : 1-6.

39. Schaffer, G.B., Sercombe, T.B., Lumley, R.N. 2001. "Liquid Phase Sintering of Aluminium Alloys." **Materials Chemistry and Physics**. 67 : 85-91.

40. Schaffer, G.B., Hall, B.J. 2002. "The Influence of the Atmosphere on the Sintering of Aluminium." **Metallurgical and Materials Transactions**. 33A : 3279-3284.

41. Schaffer, G.B. 2004. "Powder Processed Aluminium Alloys." 65-74. In Nie, J.F., Morton, A.J., Muddle, B.C. **Materials Forum**. 28 : Institute of Materials Engineering Australasia Ltd.

42. Schaffer, G.B., Hall, B.J., Bonner, S.J., Hou, S.H., Sercombe, T.B. 2006. "The Effects of the Atmosphere and the Role of Pore Filling on the Sintering of Aluminium." **Acta Materialia**. 54 : 131-138.

43. Schaffer, G.B., Yao, J.-Y., Bonner, S.J., Crossin, E., Pas, S.J., Hill, A.J. 2008. "The Effect of Tin and Nitrogen on Liquid Phase Sintering of Al-Cu-Mg-Si Alloys." **Acta Materialia**. 56 : 2615-2624.

44. Sercombe, T.B. 1998. "Non-Conventional Sintered Aluminium Alloys." Ph.D. Thesis of The University of Queensland.

45. Sercombe, T.B., Schaffer, G.B. 1999. "On the Use of Trace Additions on Sn to Enhance Sintered 2xxx Series Al Powder Alloys." **Materials Science and Engineering**. 268A : 32-39.

46. Sercombe, T.B. 2003. "On the Sintering of Uncompacted, Pre-Alloyed Al Powder Alloys." **Materials Science and Engineering**. 341A : 163-168.

47. Showaiter, N., Youseffi, M. 2007. "Compaction, Sintering and Mechanical Properties of Elemental 6061 Al Powder with and without Sintering Aids." **Materials and Design** : 1-11.

REFERENCES (CONT.)

48. Takahashi, K., interviewed on September 15, 2008. **Oxide Analysis by Using SEM and EDS Analysis.** The Office of Tokyo Institute of Technology in Thailand.

49. Tan, L.-K., Ma, J. 2004. "Performance of Powder Injection Molding (PIM) Heat Sink." in the Ninth Intersociety Conference on Thermal and Thermomechanical Phenomena in Electronic Systems. 1 : 451-454.

50. Thummler, F., Oberacker, R. 1988. **An Introduction to Powder Metallurgy**. London : The Institute of Materials.

51. Tomolya, K., Gacsi, Z., Kovacs, A. 2005. "Copper Coating by Electroless Process for Aluminium Matrix Composite." **Materials Science Forum**. 473-474 : 159-164.

52. Vukcevic, M., Delijic, K. 2002. "Some New Directions in Aluminium-Based PM Materials for Automotive Applications." **Materiali In Tehnologije**. 36 (3-4) : 101-105.

53. Warmuzek, M. 2004. Metallographic Techniques for Aluminium and Its Alloys." In Vander Voort, G.F. **ASM Handbook: Metallography and Microstructures**. 9. Ohio : ASM International.

54. Xie, G., Ohashi, O., Song, M., Mitsuishi, K., Furuya, K. 2005. "Reduction Mechanism of Surface Oxide Films and Characterization of Formations on Pulse Electric-Current Sintered Al-Mg Alloy Powders." **Applied Surface Science**. 241 : 102-106.

55. Yilmaz, M., Altintas, S. 1996. "Production of Hypereutectic Al-Si Alloys by P/M Route." **Material Science Forum**. 217-222 : 1853-1858.

56. Youseffi, M., Showaiter, N., Martyn, M.T. 2006. "Sintering and Mechanical Properties of Prealloyed 6061 Al Powder with and without Common Lubricants and Sintering Aids." **Powder Metallurgy**. 49 (1) : 86-95.

APPENDIX A

MATERIAL AND PROCESSING INFORMATION

Appendix A-1: Product information of ECKA Alumix 231

Appendix A-1: Product information of ECKA Alumix 231

ECKA ALUMIX® 231

Press-Ready Mix for Aluminium Sintered Parts

Especially for sintered parts exhibiting high wear resistance, these press-ready mix with high Silicon content was developed. Sintered parts, made of ECKA ALUMIX® 231 are showing good mechanical properties at room temperature and also at temperatures up to 200°C. Cause of the high silicon content, the CTE is reduced and therefore an application by using different materials is interesting.

Physical characteristics		Chemical compositions	
Apparent density	1,05 - 1,25 g/cm³	Aluminium	Remainder
Tap density	1,20 - 1,50 g/cm³	Silicon	14 - 16 %
Sieve fraction < 45 µm	25 - 40 %	Copper	2,4 - 2,8 %
		Magnesium	0,50 - 0,80 %

Lubricant: 1,5 % Amidwax

Recommended Compacting and Sintering Conditions:			
Compacting:	Compacting Pressure:	620 MPa →	Green density: 2,48 g/cm³
Sintering:	Dewaxing:	380 - 420°C or direct on sintering temperature	
	Sintering temperature:	550 - 560°C	
	Sintering time:	approx. 60 min	
	Atmosphere:	N_2, dew point < -45°C	

The tolerance accuracy of the sintered parts can be increased by calibration; T_6 treatment is recommended to improve material properties.

Typical Material Properties[1] of ECKA ALUMIX® 231 Sintered Parts
(Green density: 2,48 g/cm³)

Sintered density	Dim. change		Tensile strength	Hardness HB	Elongation A5
2,67 g/cm³	-2,0 %	T_{1a}	200 N/mm²	100	1 %
		T_4	280 N/mm²	130	0,5 %

[1] The results refer to MPa-test bars, sintered at laboratory conditions.

More detailed information is included in our technical brochure "ECKA ALUMIX" or please contact our service team for further information.

Contact:
ECKA Granulate Velden GmbH

Herr Hans-Claus Neubing
D-91235 Velden
Germany
Tel.: (+49) (9152) 9211-802
Fax: (+49) (9152) 9211-809
e-mail: h.neubing@ecka-granules.com

ecka granules®
Metal-Powder-Technologies

Figure A-1 Scanned image of product information of aluminium alloy powder used in this study.

BIOGRAPHY

Name: Mr. Atsawin Salee

Date of Birth: March 14, 1985

Place of Birth: Bangkok, Thailand

Education:

2003-2007	B. Sc. in Physics (1st class honour), Department of Physics, Faculty of Science, King Mongkut's University of Technology Thonburi (KMUTT)
2007-2009	M. Eng. in Automotive Engineering (International program), International College, King Mongkut's Institute of Technology Ladkrabang (KMITL)

Honour and Scholarships:

2003-2007	Full scholarship for study in the bachelor degree from Faculty of Science, KMUTT
2007	Received B. Sc. with the 1st class honour in Physics
2007-2009	Full scholarship for study in the master degree from National Science and Technology Development Agency (NSTDA)

Publications:

1. A. Salee, A. Manonukul, C. Thianpong, and K. Takahashi. "Improving Sinterability of Aluminium Alloy (Al-Si-Cu-Mg) by Adjusting Sintering Conditions." **Thammasat International Journal of Science and Technology**. In Press. (This has been selected as 1 of 18 manuscripts from 80 manuscripts in the Proceeding of the 2nd Thammasat University International Conference on Chemical, Environmental and Energy Engineering)
2. A. Salee, A. Manonukul, C. Thianpong, and K. Takahashi. "Improving Sinterability of Aluminium Alloy (Al-Si-Cu-Mg) by Adjusting Sintering Conditions." **Proceeding of the 2nd Thammasat University International Conference on Chemical, Environmental and Energy Engineering,** Bangkok, Thailand, March 3-4, 2009. pp 226-231.